

# The interplay of coordinative, hydrogen bonding and $\pi$ – $\pi$ stacking interactions in sustaining supramolecular solid-state architectures. A study case of bis(4-pyridyl)- and bis(4-pyridyl-*N*-oxide) tectons

Herbert W. Roesky<sup>a,\*</sup>, Marius Andruh<sup>b,1</sup>

<sup>a</sup> *Institut für Anorganische Chemie der Universität Göttingen, Tammannstr. 4, D-37077 Göttingen, Germany*

<sup>b</sup> *Inorganic Chemistry Laboratory, Faculty of Chemistry, University of Bucharest, Str. Dumbrava Rosie nr. 23, 70254 Bucharest, Romania*

Received 25 February 2002; accepted 9 August 2002

## Contents

Abstract	91
1. Introduction	91
2. Hydrogen bonds and $\pi$ – $\pi$ stacking interactions—useful tools in crystal design	92
3. The classical molecular rod in constructing supramolecular polymetallic architectures: 4,4'-bipyridine	94
4. The [4,4'-H <sub>2</sub> bipy] <sup>2+</sup> tecton: organic–inorganic hybrid materials constructed from MX <sup>+</sup> ·HN <sup>+</sup> synthons	103
5. 4,4'-Bipyridine- <i>N,N'</i> -dioxide—a new tecton in crystal engineering	105
6. A flexible <i>N,N'</i> - <i>exo</i> -bidentate ligand: 1,2-bis(4-pyridyl)ethane	111
7. Conclusions and perspectives	116
Acknowledgements	117
References	117

## Abstract

Bis-monodentate ligands, such as bis(4-pyridyl) derivatives and bis(4-pyridyl-*N*-oxide), are able to generate polymetallic coordination networks with interesting supramolecular solid-state architectures. This review is devoted to high-dimensionality systems, which are extended by combining two or three organizing forces: metal-coordination, hydrogen bonds and  $\pi$ – $\pi$  stacking interactions. A special emphasis is given to the following molecules, which play the role of linkers and spacers in the construction of extended frameworks: 4,4'-bipyridine, 1,2-bis(4-pyridyl)ethane, *trans*-1,2-bis(4-pyridyl)ethene, *trans*-4,4'-azo-pyridine, 4,4'-bipyridyl-*N,N'*-dioxide.

© 2002 Elsevier Science B.V. All rights reserved.

**Keywords:** Extended structures; Coordination polymers; Stacking interactions; Hydrogen bonds; Crystal engineering

## 1. Introduction

In the past decade, the crystal design and engineering of multidimensional arrays and networks containing metal ions as nodes have achieved considerable progress. The increasing interest in this field, which involves

both synthetic and theoretical chemists, physicists, crystallographers and materials scientists, is justified by the potential utility of these compounds as zeolite-like materials [1], catalysts [2] or magnetic materials [3]. There is also an aesthetic perspective: chemists are attracted by the particular beauty and the intriguing diversity of the structures which can be obtained by assembling metal ions and various multifunctional ligands. Although numerous beautiful compounds illustrate reliable predictions of the solid-state architectures, many other interesting structures could not be predicted.

\* Corresponding author. Tel.: +49-551-393001

E-mail addresses: hroesky@gwdg.de (H.W. Roesky), marius.andruh@dent.ro (M. Andruh).

<sup>1</sup> Also corresponding author. Tel.: +40-744-870656

However, their retrospective analysis provides the necessary information in the attempt to design intentionally inorganic or organic/inorganic hybrid materials with specific functions and properties.

Two components are necessary in every synthetic approach leading to extended supramolecular multi-metallic assemblies: the ligand (the organic tecton) and the metal ion. In the language of supramolecular chemistry, the ligand is a programmed species, whose information is read by the metal ions according to their coordination algorithm (stereochemical preference) [4]. The coordination geometry of the metal ion is then crucial in self-assembly processes. Of course, the solvent molecules and the counterions influence also the final supramolecular architecture. The non-coordinating anions play not only a charge-compensating role, but they can dramatically influence the overall solid-state architecture through their templating function.

Since the pioneering work of Robson and co-workers in 1990 [5], *exo*-bidentate (divergent) ligands such as pyrazine or 4,4'-bipyridine (4,4'-bipy) are widely used as building blocks in designing coordination polymers (the so-called 'node and spacer' approach). The stoichiometry of divergent ligand:metal is a key factor in determining the dimensionality of the resulting systems. A 1:1 ligand-to-metal ratio leads to either linear or zigzag chains [6]. By altering the stoichiometry, namely by increasing the ligand-to-metal ratio, 2- and 3-D architectures can be obtained. In this case, the structures are expanded either through supplementary metal-bridging ligand bonds, or through the cooperation of coordinative, hydrogen bonds and  $\pi$ - $\pi$  stacking interactions. The formation of 1-D chains is favored by the presence of ancillary ligands in the coordination sphere of the metal ion, whereas 2- or 3-D structures are obtained by using 'naked' (actually hydrated) cations. If the 2- or 3-D extended structures are based only on the metal-coordination, the resulting network topology is directly influenced by the coordination geometry of the metal ions (templates). So, for a 2:1 L-M stoichiometry, diamondoid networks are obtained by using Ag(I) or Cu(I) as assembling cations, both with a marked preference for the tetrahedral coordination [7], while square grid networks are obtained by using as templates metal ions, which can easily adopt the octahedral stereochemistry [8]. These systems are covered by some recent excellent reviews [9].

In this review we will focus on high-dimensionality systems constructed by combining two or three organizing forces: metal-coordination, hydrogen bonds and  $\pi$ - $\pi$  stacking interactions (Scheme 1). These are extremely useful tools in supramolecular chemistry and crystal engineering. Their interplay will be illustrated by representative examples chosen from the chemistry generated by bis(4-pyridyl)- and bis(4-pyridyl-*N*-oxide) divergent ligands (Scheme 2).

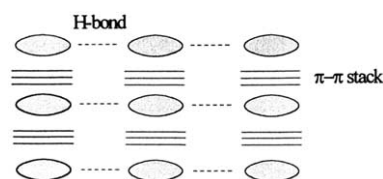
## 2. Hydrogen bonds and $\pi$ - $\pi$ stacking interactions—useful tools in crystal design

Hydrogen bonding, one of the better understood types of non-covalent interactions [10], is a powerful organizing force in designing solids for several reasons: it is directional, selective and its formation is reversible at room temperature [11]. As noted by Zaworotko [9e], the 'node and spacer' approach, which involves metal ions and *exo*-bidentate ligands, can be applied with hydrogen bonds as well. Indeed, in many respects, hydrogen bonds can be compared with metal-ligand coordinate bonds: together with its directionality, the interaction between the protic hydrogen atom (arising from the donor, D-H) and the region of higher electronic density of the acceptor (:A) is similar to the metal-ligand interaction. Hydrogen bonds are extensively used for networking numerous organic and organometallic compounds [11].

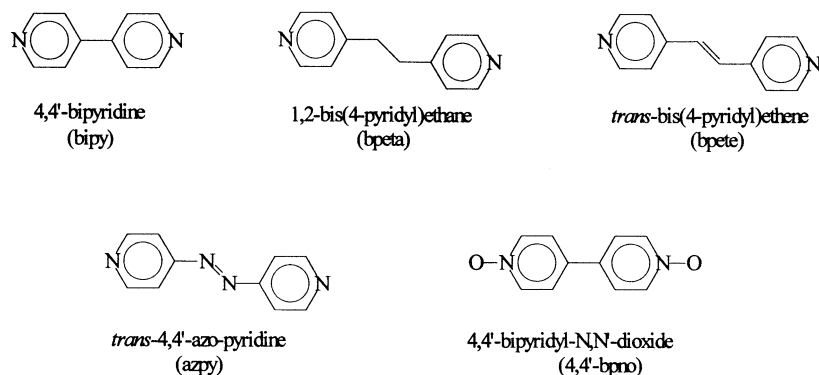
The other non-covalent forces with an important role in self-assembly and molecular recognition processes are the aromatic-aromatic ( $\pi$ - $\pi$  stacking) interactions [12]. They are weakly directional and weaker than the hydrogen bonds: calculations give about 10 kJ mol<sup>-1</sup> [13] (for typical aromatic-aromatic interactions), in comparison with 15–40 kJ mol<sup>-1</sup> (for moderate hydrogen bonds between neutral molecules). Ring stacking may enhance the stability of metal complexes both in solution and in solid-state.

At the supramolecular level, the aromatic rings can interact in different ways: stacked arrangement (face-to-face, perfect alignment, and offset, slipped, parallel displaced) and edge- or point-to-face, T-shaped conformation (Scheme 3). The last one results from C-H $\cdots\pi$  interactions. The facial arrangements are particularly important for the case of the ligands containing pyridyl moieties. A very useful critical review, dealing with aromatic-aromatic interactions in metal complexes, has been recently published by Janiak [14].

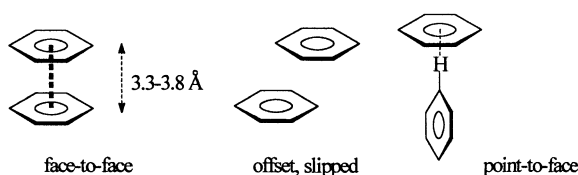
Mononuclear complexes containing aromatic ligands can be assembled into various supramolecular architectures by means of  $\pi$ - $\pi$  interactions of the aromatic rings. The number of the aromatic moieties, as well as their spatial arrangement are important factors in determining the dimensionality of the extended structure. For example, in the case of mononuclear monochelated complexes containing 2,2'-bipyridine or 1,10-phenanthroline, the aromatic-aromatic stacking usually



Scheme 1.



Scheme 2.

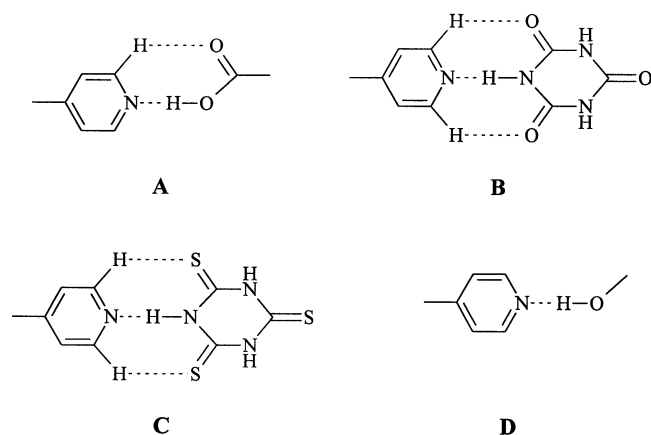


Scheme 3.

gives pairs of interacting mononuclear complexes [15], while the bis-chelated mononuclear complexes, with similar ligands, are assembled into 1-D chains [16]. The increase of the number of the aromatic moieties which can interact results in a higher dimensionality [17].

Let us illustrate, separately, the role of hydrogen bonding and of stacking interactions in generating supramolecular solid-state architectures.

4,4'-Bipyridine is able to generate not only polynuclear complexes, but also supramolecular organizations with various organic molecules. Most frequently, 4,4'-bipy acts as hydrogen bond acceptor, although it can be a hydrogen bond donor also. The self-assembly process between 4,4'-bipy and organic or organometallic molecules with exodentate functionality (trimesic acid [18a], melamine [18b], trithiocyanuric acid [18c], cyanuric



Scheme 4.

acid [18d], cubane-like clusters  $[M(CO)_3(\mu_3-OH)]_4$ ,  $M = Mn, Re$  [18e] led to robust hydrogen bonded supramolecular aggregates constructed from various synthons (Scheme 4). For example, the cocrystallization of cyanuric acid with 4,4'-bipy in water gives a 1:1 adduct (in methanol a 2:1 adduct is formed) [18d]. In the 1:1 adduct, the cyanuric acid molecules are held together in chains by single  $N-H \cdots O$  hydrogen bonds ( $H \cdots O$ , 2.02 Å); these chains are further interconnected by the 4,4'-bipy molecules through  $N-H \cdots N$  bonds ( $H \cdots N$ , 1.92, 1.94 Å), resulting in layers (Fig. 1). Adjacent layers are aligned parallel to each other without interpenetration.

The next example, which illustrates the formation of supramolecular motifs by means of aromatic–aromatic interactions, has the beauty of a textbook case. The reaction between Cu(I) ions and 1-aminopyrene (apyr) affords mononuclear cations,  $[Cu(apyr)_3]^+$ , in which the copper atom has a coordination number of three [17b].

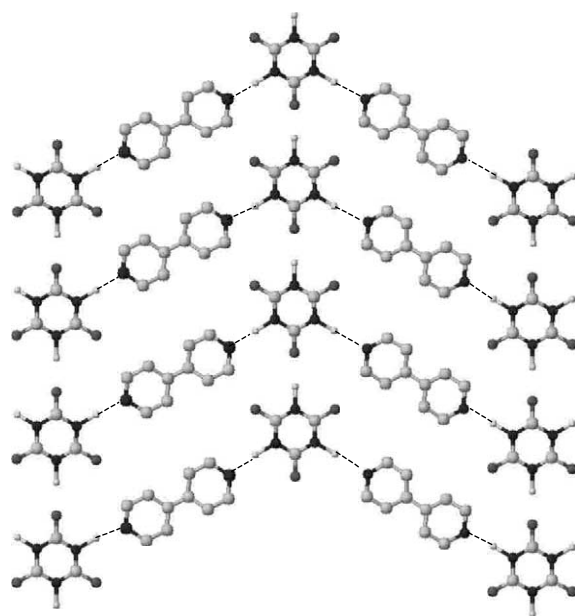


Fig. 1. A 2-D layer resulted from cyanuric acid and 4,4'-bipy in the 1:1 hydrogen bonded adduct (adapted from Ref. [18d]).

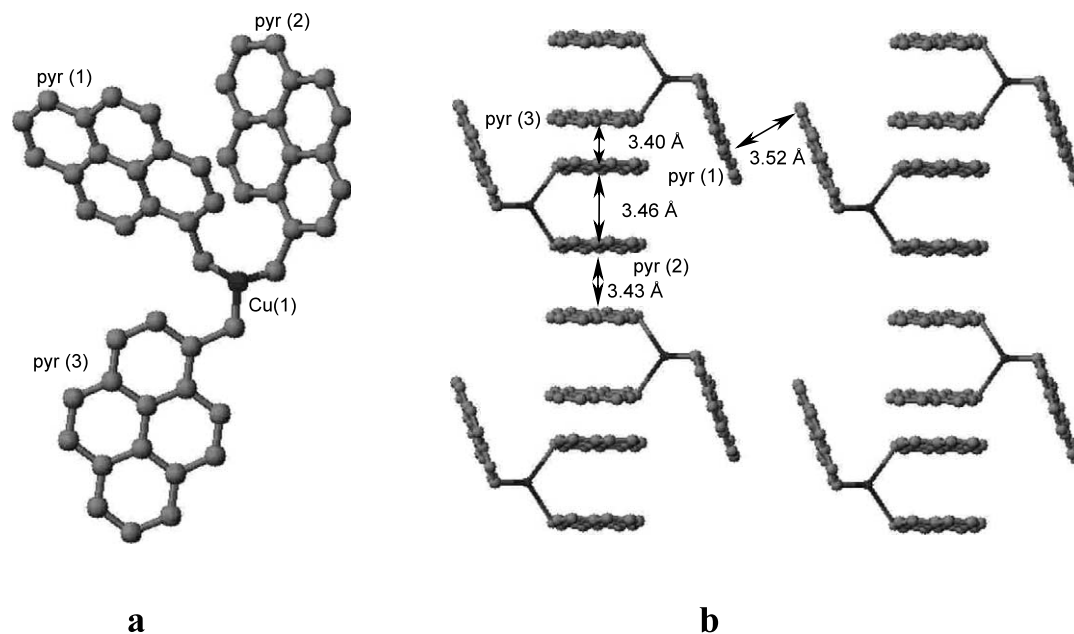


Fig. 2. (a) Molecular structure of the  $[\text{Cu}(\text{apyr})_3]^+$  cation; (b) diagram showing the layers formed by intermolecular stacking interactions between the pyrene (pyr) moieties (adapted from Ref. [17b]).

There are intra- and intermolecular  $\pi$ – $\pi$  interactions of the three pyrene moieties; the last ones generate a 2-D layer (Fig. 2).

Another interesting case is that of  $[\text{Ag}(\text{azpy})(\text{NO}_3)] \cdot \text{H}_2\text{O} \cdot \text{CH}_3\text{OH}$  (azpy = *trans*-4,4'-azopyridine). The Ag(I) ions are bridged by azpy ligands, resulting in infinite chains. Pairs of chains are linked together by  $\pi$ – $\pi$  stacks between the azpy ligands (with a distance of 3.53 Å) (Fig. 3). The distance between the silver atoms is also quite short (3.30 Å) [19].

It is worth mentioning that the non-covalent interactions lead not only to various supermolecules and solid-state architectures, but generate also interesting supramolecular properties, such as electrical, optical and magnetic ones [20]. They are responsible for many cooperative phenomena in molecular solids. Furthermore, the cooperativity may lead to thermal hysteresis, which confers a memory effect to a magnetic material [20a,20b]. The stacking interactions were found able to

mediate both antiferro- and ferromagnetic couplings [20c,20d].

### 3. The classical molecular rod in constructing supramolecular polymetallic architectures: 4,4'-bipyridine

4,4'-Bipyridine is among the most popular ligands used in designing metal coordination networks [9]. It can act as bridging and terminal ligand, but can be found in solid-state as an uncoordinated guest molecule as well. The terminal and uncoordinated 4,4'-bipy molecules may be further involved in either hydrogen bond or stacking interactions (Scheme 5). The solid-state architecture of the metal–4,4'-bipy systems is strongly dependent on: (1) the metal-to-ligand molar ratio; (2) the function accomplished by 4,4'-bipy (bridging, terminal, uncoordinated); (3) the stereochemical preference of the metal ion; (4) the presence of solvent molecules

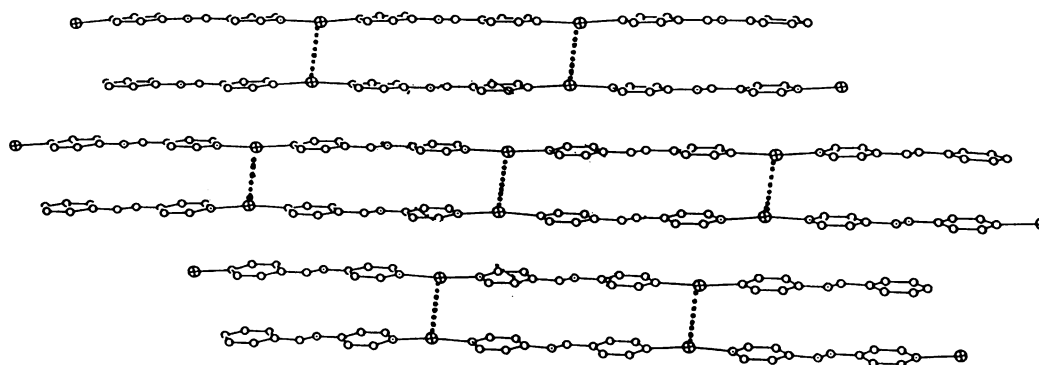
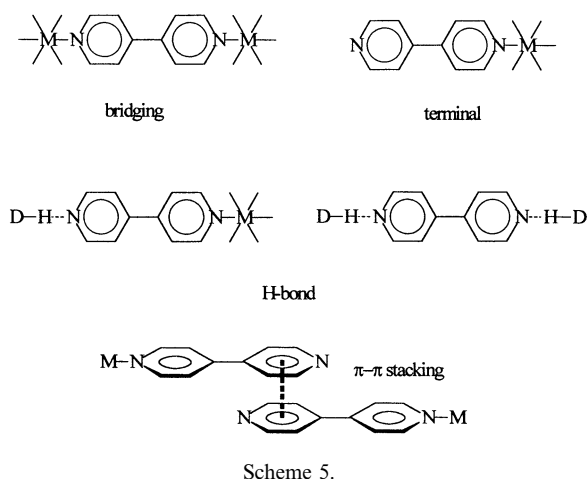


Fig. 3. Pairs of linear chains in  $[\text{Ag}(\text{azpy})(\text{NO}_3)] \cdot \text{H}_2\text{O} \cdot \text{CH}_3\text{OH}$ , resulted from  $\pi$ – $\pi$  and  $\text{Ag} \cdots \text{Ag}$  interactions (adapted from Ref. [19]).



acting as ligands and as possible hydrogen bond donors, D–H, towards the terminal or uncoordinated 4,4'-bipy molecules; (5) the role of the anions (coordinated, bridging, uncoordinated); (6) the presence of organic guest molecules.

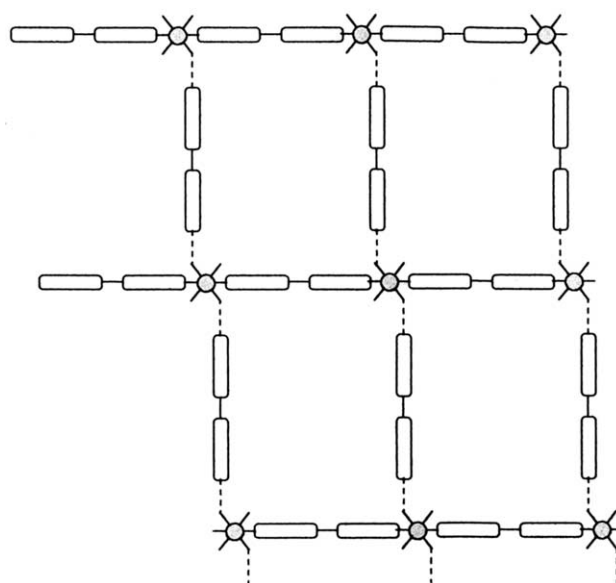
As already stated, the 1:1 metal-to-ligand ratio leads only to chains (linear or zigzag). For the 1:1.5 ratio, the following architectures are based solely on metal–ligand coordinative interactions: molecular ladder, molecular brick wall, honeycomb, molecular bilayer [9]. The 1:2 metal-to-ligand molar ratio is more interesting for the purpose of this review. If the two 4,4'-bipy molecules act as bridging ligands, then the following extended structures can be constructed: square grid and diamondoid [9]. If only one 4,4'-bipy molecule acts as a bridge, whereas the other one is uncoordinated, two types of systems have been characterized so far:

$[M(4,4'\text{-bipy})(H_2O)_4]X_2 \cdot (4,4'\text{-bipy})$  (1:  $M = Zn$ ,  $X = NO_3$ ) [21];

and

$[M(4,4'\text{-bipy})(H_2O)_2X_2] \cdot (4,4'\text{-bipy})$  (2:  $M = Cu$ ,  $X = BF_4$  [22]; 3:  $M = Cu$ ,  $X = ClO_4$  [23]; 4:  $M = Cd$ ,  $X = ClO_4$  [24]; 5:  $M = Mn$ ,  $X = NCS$  [25]; 6:  $M = Fe$ ,  $X = NCS$  [26]; 7:  $M = Co$ ,  $X = NCS$  [27]).

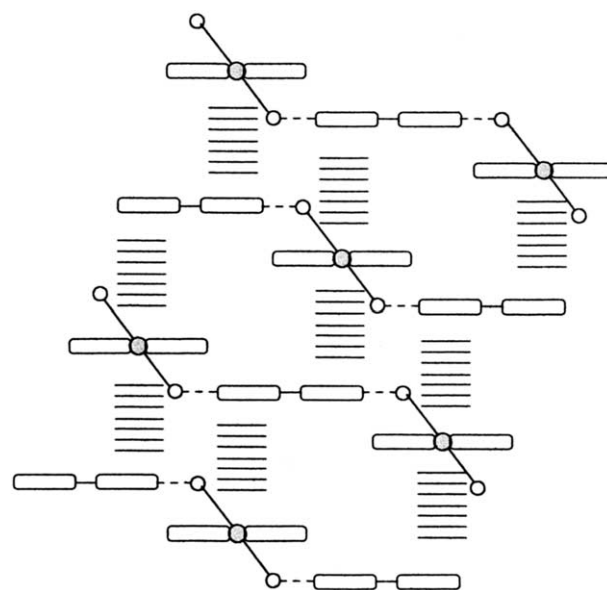
Compounds 2 and 3 are isostructural and isomorphous and crystallize in the monoclinic space group  $C2/c$ ; compounds 4, 5, 6 and 7 are isomorphous too (triclinic,  $P\bar{1}$ ). In all these compounds the metal ions exhibit a (pseudo)octahedral stereochemistry. A higher tetragonal distortion is found, as expected, with the Cu(II) ions in compounds 2 and 3, due to the intervening Jahn–Teller effect. The crystal structures of compounds 1–7 have two common features: (a) one 4,4'-bipy molecule bridges metal atoms directly, resulting in infinite M–4,4'-bipy–M linear chains, all running in a parallel direction; (b) the uncoordinated 4,4'-bipy molecule, acting as a spacer, is hydrogen bonded and bridges the coordinated water molecules arising from two nearest neighboring chains. Linear M–bipy–M and zigzag M–OH<sub>2</sub>··bipy··H<sub>2</sub>O–M chains form a stair-



Scheme 6.

type connection resulting in 2-D layers of rhombic meshes (Scheme 6). The M···M distances via coordinate bonds range from 11.1 to 11.5 Å, while those involving hydrogen bonds are longer, ranging between 14.9 and 15.8 Å.

The tertiary structure for these compounds is achieved in different ways. In compounds 2 and 3 the layers are interconnected by hydrogen bonds involving the aqua ligands and the  $ClO_4^-$  or  $BF_4^-$  anions, resulting in a network with rhomboidal cavities. In compounds 5–7, the interconnection between neighboring layers is made through stacking interactions between the coordinated 4,4'-bipy from one layer and uncoordinated ones arising from the adjacent layers lying above and below (Scheme



Scheme 7.



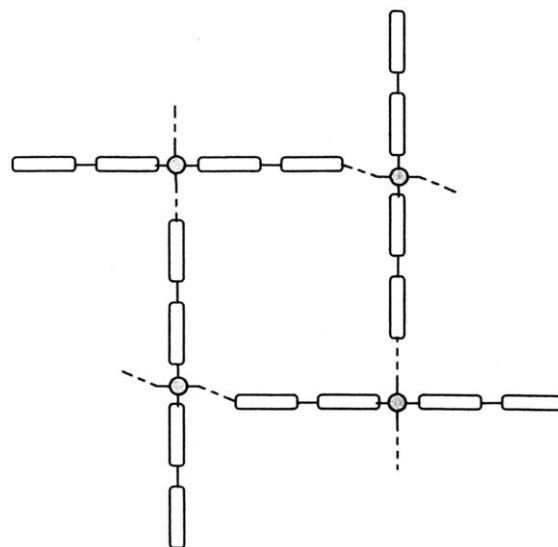
7). The separation between 4,4'-bipy molecules in **6** is about 3.43 Å. Similar stacking interactions are found in compounds **2** and **3** (ca. 3.50 Å in **2**). Compounds **2–7** do not show interpenetration.

The tertiary structure of compound **1** is different: the two other *trans*-aqua ligands, which are not involved in the in-layer hydrogen bonds, give Zn–OH<sub>2</sub>⋯(NO<sub>3</sub><sup>−</sup>)<sub>2</sub>⋯H<sub>2</sub>O–Zn bridges linking the next nearest layer. A system of two interpenetrating nets, topologically related to α-polonium, is formed (Fig. 4).

The structural motif depicted in Scheme 6 is found also in some compounds with other rigid bis(4-pyridyl) ligands: [Mn(bpete)(NCS)<sub>2</sub>(CH<sub>3</sub>OH)<sub>2</sub>]·(bpete) (bpete = *trans*-1,1-bis(4-pyridyl)ethene) [28], [Fe(azpy)(NCS)<sub>2</sub>(CH<sub>3</sub>OH)<sub>2</sub>]·(azpy) (azpy = *trans*-4,4'-azo-pyridine) [26]. These two compounds are isostructural and isomorphous (monoclinic, *P*2<sub>1</sub>/*c*).

Finally, both 4,4'-bipy molecules can act as terminal ligands. Such compounds have been obtained by reacting oxalato-bridged heteropolynuclear complexes of the type [MCr<sub>2</sub>(AA)<sub>2</sub>(C<sub>2</sub>O<sub>4</sub>)<sub>4</sub>(H<sub>2</sub>O)<sub>*n*</sub>] (AA = 2,2'-bipy or 1,10-phen; M = Mn, *n* = 0; M = Co, Ni, Zn, *n* = 2) with 4,4'-bipy. The resulting compounds have the formula [M(4,4'-bipy)<sub>2</sub>(H<sub>2</sub>O)<sub>4</sub>][Cr(AA)(C<sub>2</sub>O<sub>4</sub>)<sub>2</sub>]<sub>*n*</sub>·*n* H<sub>2</sub>O (**8**), where both cation and anion are mononuclear complex species [29]. Each peripheral pyridyl moiety from the [M(4,4'-bipy)<sub>2</sub>(H<sub>2</sub>O)<sub>4</sub>]<sup>2+</sup> cations is hydrogen bonded to the aqua ligands from other similar species (Scheme 8), generating 2-D layers with rhombic meshes.

If the self-assembly process between metal salts and 4,4'-bipy is carried out in the presence of organic guest molecules, 2-D square grid coordination networks are obtained, that is, the connection of the metal ions is solely made through 4,4'-bipy bridges. The organic molecules are clathrated in the square cavities (Table



Scheme 8.

Table 1

Host–guest system	Guest molecule	Reference
Cd(4,4'-bipy) <sub>2</sub> (NO <sub>3</sub> ) <sub>2</sub> ·2G ( <b>9</b> )	<i>o</i> -Dibromobenzene	[2]
Cd(4,4'-bipy) <sub>2</sub> (ClO <sub>4</sub> ) <sub>2</sub> ·2G·G' ( <b>10</b> )	<i>o</i> -Nitroaniline (G), 4,4'-bipy (G')	[24]
Cd(4,4'-bipy) <sub>2</sub> (ClO <sub>4</sub> ) <sub>2</sub> ·2G ( <b>11</b> )	<i>N</i> -Methyl- <i>o</i> -nitroaniline	[24]
Cd(4,4'-bipy) <sub>2</sub> (H <sub>2</sub> O) <sub>2</sub> (ClO <sub>4</sub> ) <sub>2</sub> ·2G ( <b>12</b> )	2,4'-Bipyridine	[30a]
Zn(4,4'-bipy) <sub>2</sub> (H <sub>2</sub> O) <sub>2</sub> (ClO <sub>4</sub> ) <sub>2</sub> ·2G ( <b>13</b> )	2,4'-Bipyridine	[30a]
[Cu(4,4'-bipy) <sub>2</sub> (H <sub>2</sub> O) <sub>2</sub> (ClO <sub>4</sub> ) <sub>4</sub> ] <sup>2−</sup> ·G ( <b>14</b> )	4,4'-H <sub>2</sub> bipy <sup>2+</sup>	[30a]
Ni(4,4'-bipy) <sub>2</sub> (NO <sub>3</sub> ) <sub>2</sub> ·2G ( <b>15</b> )	Pyrene	[31]

1) [2,24,30,31]. The guest molecules are stabilized in the host cavities by aromatic–aromatic stacking and/or hydrogen bonding interactions. The incorporation of non-linear optical-active guests into 2- or 3-D coordination polymers is expected to lead to interesting NLO materials [24].

The crystallographic investigation of the host–guest system {[Ni(4,4'-bipy)<sub>2</sub>(NO<sub>3</sub>)<sub>2</sub>]·2(pyrene)}<sub>*n*</sub> (**15**) reveals a very interesting case of complementary, interpenetrating covalent and non-covalent networks [31]. The 2-D square grid coordination networks possess inner cavities of ca. 8 × 8 Å and stack parallel to one another. The interconnection between the grids is made by C–H⋯O hydrogen bond interactions established between 4,4'-bipy ligands and nitrate anions of adjacent grids (the C⋯O separations are in the range 2.87–3.15 Å). The pyrene molecules are organized in 2-D layers, which are sustained by edge-to-face interactions. The shortest intermolecular C⋯C distance is 3.518 Å. The pyrene nets thread orthogonally with the coordination nets, via face-to-face interactions with the 4,4'-bipy ligands (the

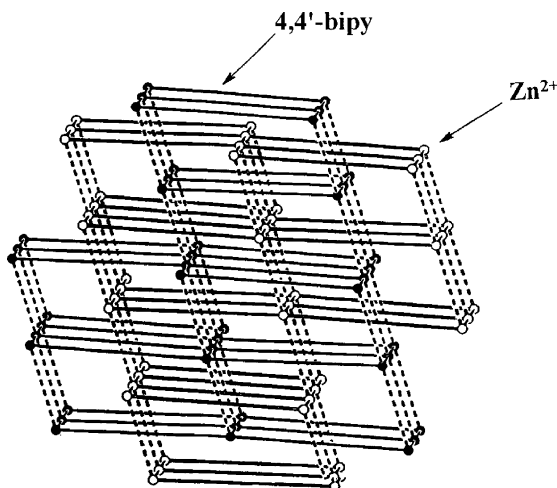


Fig. 4. Two interpenetrating networks in compound **1**. The rods represent the 2-D layers resulting from M–OH<sub>2</sub>⋯bipy⋯H<sub>2</sub>O–M bridges, while the broken rods represent the hydrogen bonds involving the anions (adapted from Ref. [21]).

shortest C··C separation between 4,4'-bipy and pyrene molecules is ca. 3.4 Å, and corresponds to face-to-face stacking interactions).

Two compounds have been described for the molar ratio  $M:4,4'\text{-bipy} = 1:2.5$ :  $[\text{Fe}(\text{bipy})(\text{H}_2\text{O})_3(\text{ClO}_4)]\text{ClO}_4 \cdot 1.5(4,4'\text{-bipy}) \cdot \text{H}_2\text{O}$  (**16**) [21] and  $[\text{Ni}(4,4'\text{-bipy})_{2.5}(\text{H}_2\text{O})_2](\text{ClO}_4)_2 \cdot 1.5(4,4'\text{-bipy}) \cdot 2\text{H}_2\text{O}$  (**17**) [32]. Formally, compound **17** belongs to the 1:4 stoichiometry, but 1.5 mol of 4,4'-bipy do not participate to the construction of the framework. The structure of **17** consists of linear railroad double chains constructed from bridging and terminal 4,4'-bipy ligands. Large pores ( $11 \times 11$  Å) are formed. The terminal organic ligands further extend the structure through  $\pi$ - $\pi$  interactions with identical terminal ligands (3.77 Å) from adjacent chains (Scheme 9, Fig. 5). The 2-D sheets are stacked in registry resulting in an extended 1-D channel network with large pores along the crystallographic *a* axis. Although such networks have the tendency to self-include, compound **17** shows no interpenetration. The pores are occupied by hydrogen bonded hydrated anions and 4,4'-bipy guests which avoid interpenetration.

Compounds exhibiting this type of solid-state architecture are very good candidates for ion-exchange processes. The elimination of the guest water molecules results in a higher mobility of the guests anions, which can be exchanged with other ions, without destruction of the network. Indeed, a dehydrated sample of **17**, immersed in an aqueous solution containing  $\text{NaPF}_6$ , exchanges the perchlorate anions with  $\text{PF}_6^-$  anions. The infrared spectrum of the resulting solid clearly indicates the substitution of the  $\text{ClO}_4^-$  ions (disappearance of the intense peaks at  $1150\text{--}1091\text{ cm}^{-1}$ ) with  $\text{PF}_6^-$  ions (appearance of new intense peaks at 845 and 565

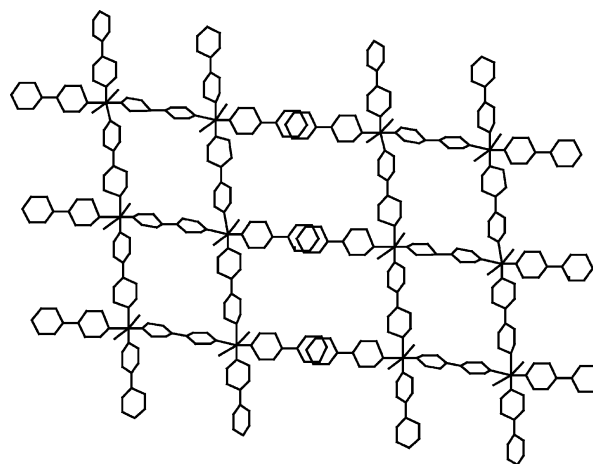
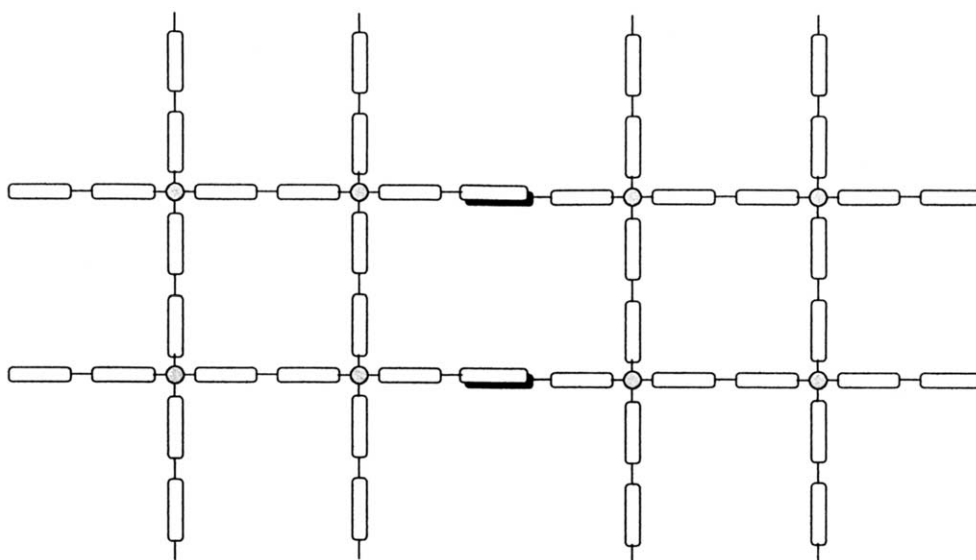


Fig. 5. The formation of a layer in compound **17** (adapted from Ref. [32]).

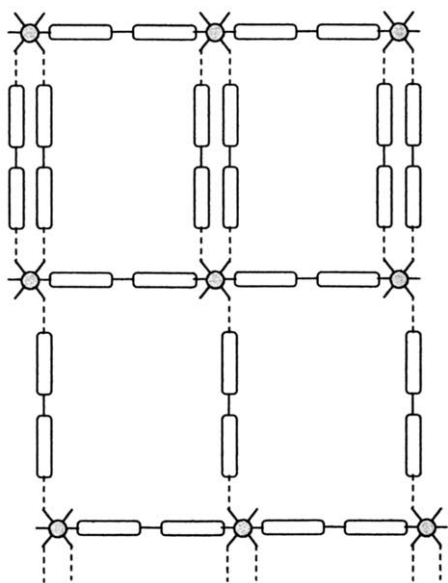
$\text{cm}^{-1}$ ), the material remaining crystalline. The robust solid-state architecture of **17** is clearly the result of the interplay of coordinative and stacking interactions.

The supramolecular architecture of compound **16** is related to the one exhibited by compounds **1–7**, with the difference that the adjacent chains are hydrogen bonded alternatively by single and double 'bridges' (Scheme 10). The interconnection of the chains by only double 'bridges' (Scheme 11) corresponds to the metal-to-ligand molar ratio 1:3. Two compounds of this type have been characterized:  $[\text{Zn}(4,4'\text{-bipy})(\text{H}_2\text{O})_4](\text{NO}_3)_2 \cdot 2(4,4'\text{-bipy}) \cdot 3\text{H}_2\text{O}$  (**18**) and  $[\text{Zn}(4,4'\text{-bipy})(\text{H}_2\text{O})_4](\text{CF}_3\text{SO}_3)_2 \cdot 2(4,4'\text{-bipy})$  (**19**) [21]. In compounds **16**, **18**, **19** the distances between the parallel bipy spacers are in the range 3.6–3.7 Å indicating rather weak stacking interactions.

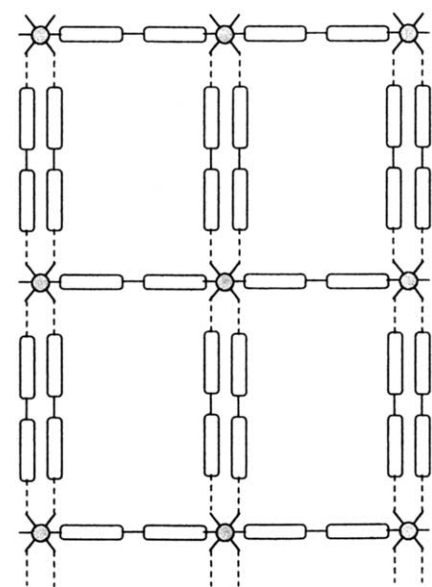
Within the 1:3 metal–bipy stoichiometry, only one other architecture has been encountered, namely in



Scheme 9.



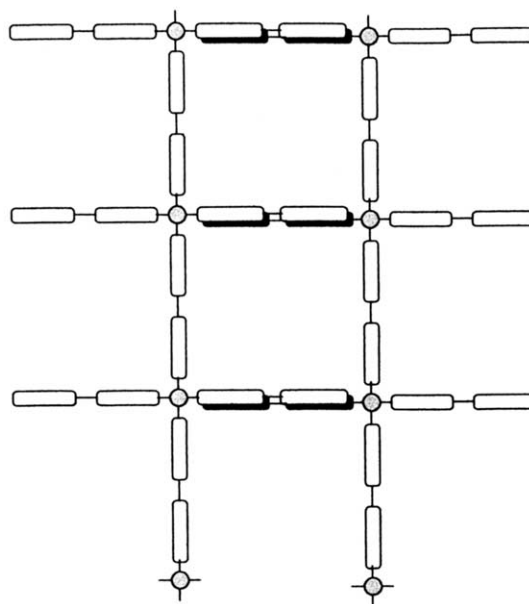
Scheme 10.



Scheme 11.

$[\text{Cd}(\text{4,4'}\text{-bipy})_3(\text{H}_2\text{O})_2](\text{ClO}_4)_2 \cdot 2\text{H}_2\text{O}$  (**20**) [24]: one bipy molecule acts as a bridge leading to linear chains, while the two others are coordinated in *trans* as terminal ligands (Scheme 12). The terminal 4,4'-bipy ligands from adjacent chains stack on top of each other.

The highest content in 4,4'-bipy, namely 1(metal):6(bipy), is found in a Mn(II) compound:  $[\text{Mn}(\text{4,4'}\text{-bipy})_2(\text{H}_2\text{O})_4](\text{ClO}_4)_2 \cdot 4(\text{4,4'}\text{-bipy})$  (**21**) [33]. All six 4,4'-bipy molecules are involved, with different roles, in the construction of the 3-D architecture. The manganese ions are hexacoordinated by two 4,4'-bipy rests, and four aqua ligands. Two 4,4'-bipy molecules are coordinated in *trans* as terminal ligands to manganese. The 3-D order is achieved by the cooperation of hydrogen



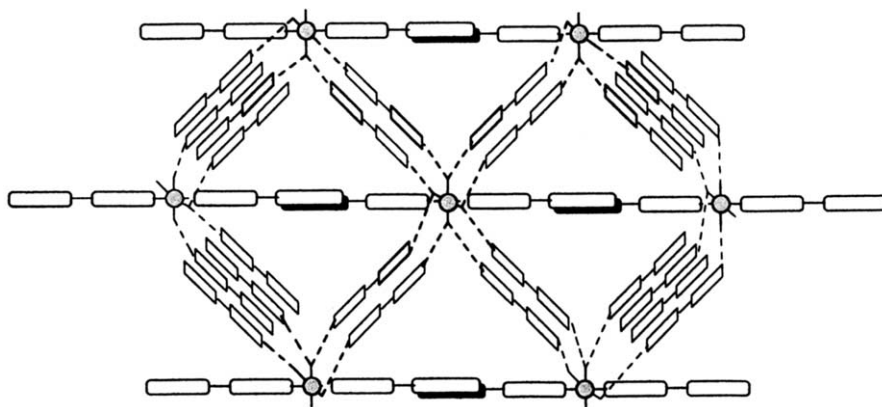
Scheme 12.

bonding and stacking interactions (Scheme 13). The terminal 4,4'-bipy ligands extend the structure via stacking interactions (face-to-face separation of ca. 3.55 Å), resulting in linear chains. The parallel chains are further interconnected through hydrogen bond interactions involving the aqua ligands and the uncoordinated 4,4'-bipy molecules. The structure can be described also as been made by triangular subunits, which result from hydrogen bond and  $\pi$ - $\pi$  interactions. Each subunit is enclosed by three mononuclear cations, four uncoordinated 4,4'-bipy molecules and two terminal ligands interacting through aromatic-aromatic stacking. The distances between the manganese atoms located in the corners are: 14.31, 14.92, 15.45 Å. The superposition of these units in the crystal generates triangular channels, which are occupied by the perchlorate anions (Fig. 6).

Interesting architectures have been obtained by combining the bridging ability of 4,4'-bipy with the one of other bridging ligands [34]: pyrazine [34a], oxalato [34b], acetato [34c], trifluoroacetato [34d], fumarato and maleato [34e], malonato [34f], pyridin-4-carboxylato [34g], dicyanamido [34h], isophthalato [34i], terephthalato [34j], dichromato [34k], nitrilotriacetato [34l], chloro [34m], tricyanomethanide [34n], phosphato [34o], sulfato [34p].

In some cases, the increase of the dimensionality through non-covalent interactions is achieved by using supplementary ligands attached to the metal ions, which are bridged by 4,4'-bipy. Two isomorphous compounds exhibiting an unprecedented supramolecular architecture have been obtained by using the *p*-hydroxybenzoate (phba) anion as an ancillary ligand [35]:  $[\text{M}_2(\text{4,4'}\text{-bipy})_3(\text{phba})_2(\text{H}_2\text{O})_3](\text{NO}_3)_2 \cdot 4\text{H}_2\text{O}$ ,  $\text{M} = \text{Cu}(\text{II})$ , and





Scheme 13.

Co(II) (**22**). In principle, the metal–4,4′-bipy molar ratio of 1:1.5 (all bipy molecules acting as bridges) leads to four architectures [36]: molecular ladder, brick wall, molecular bilayer, as well as a more complicated 3-D frame. Compounds **22** present the first structural motif, namely the molecular ladder. The phba<sup>−</sup> anions are coordinated as terminal ligands to the metal ions, forming the lateral arms (Scheme 14). The metal ions are coordinated by three nitrogen atoms from three

different 4,4′-bipy ligands, an aqua ligand and two oxygen atoms arising from the carboxylato group (unsymmetrically chelated). This ladder is similar to that encountered in compound **17**, in the latter the inner rungs and the lateral arms being identical. The tertiary structure of compound **22** is extremely interesting and is due to the intervening  $\pi$ – $\pi$  stacks between the two types of ligands. The lateral arms of each molecular ladder are threaded into the  $[M_4(4,4′\text{-bipy})_4]$  squares of adjacent

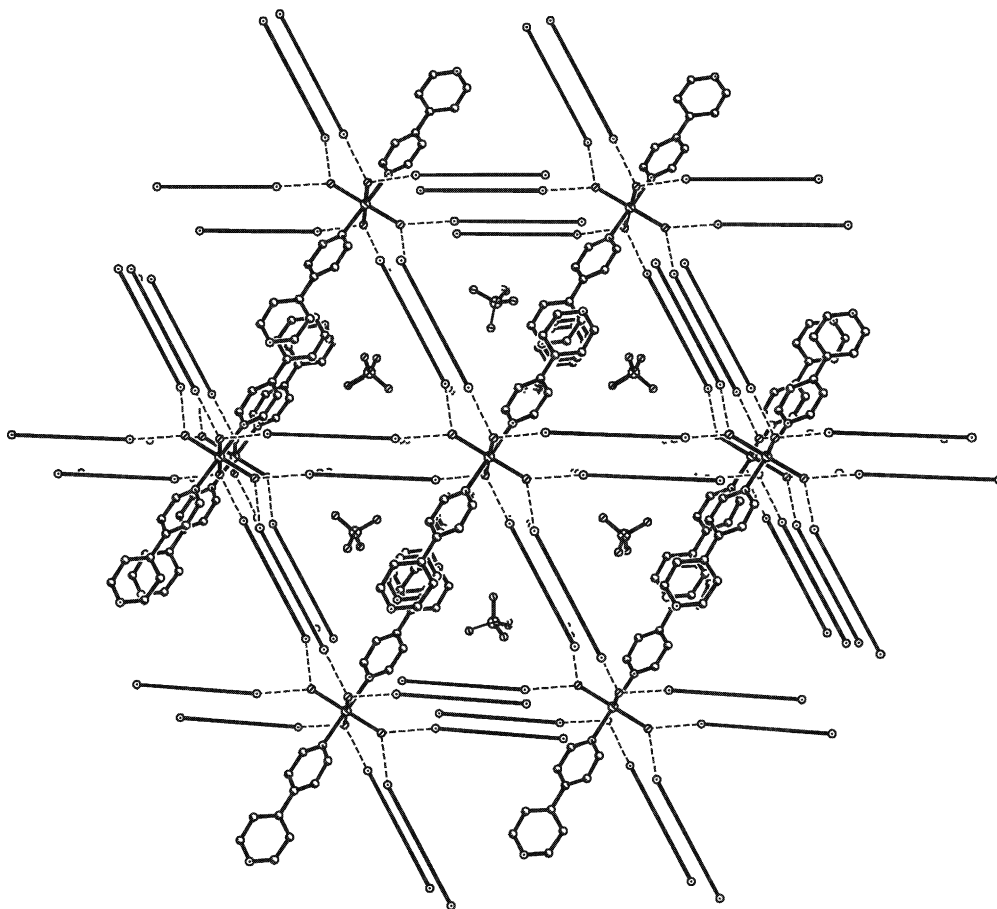
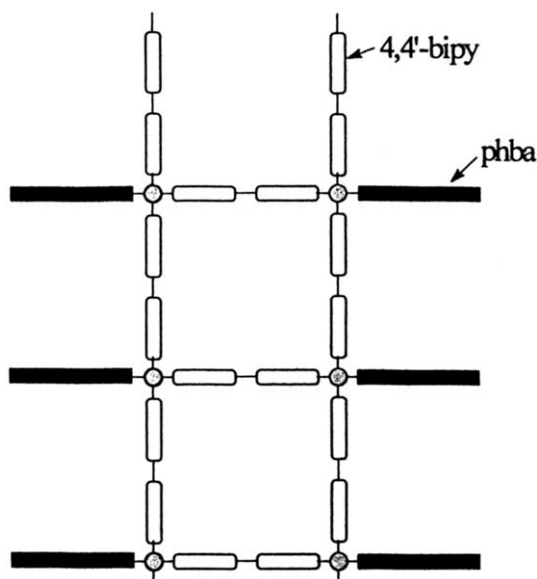


Fig. 6. View showing the triangular channels in **21**. The solvated 4,4′-bipy molecules are shown as rods. The anions have been omitted for clarity (adapted from Ref. [33]).



Scheme 14.

chains, with each square penetrated oppositely by two phba arms that belong to two different ladders (Scheme 15). The aromatic rings of the phba moieties, which

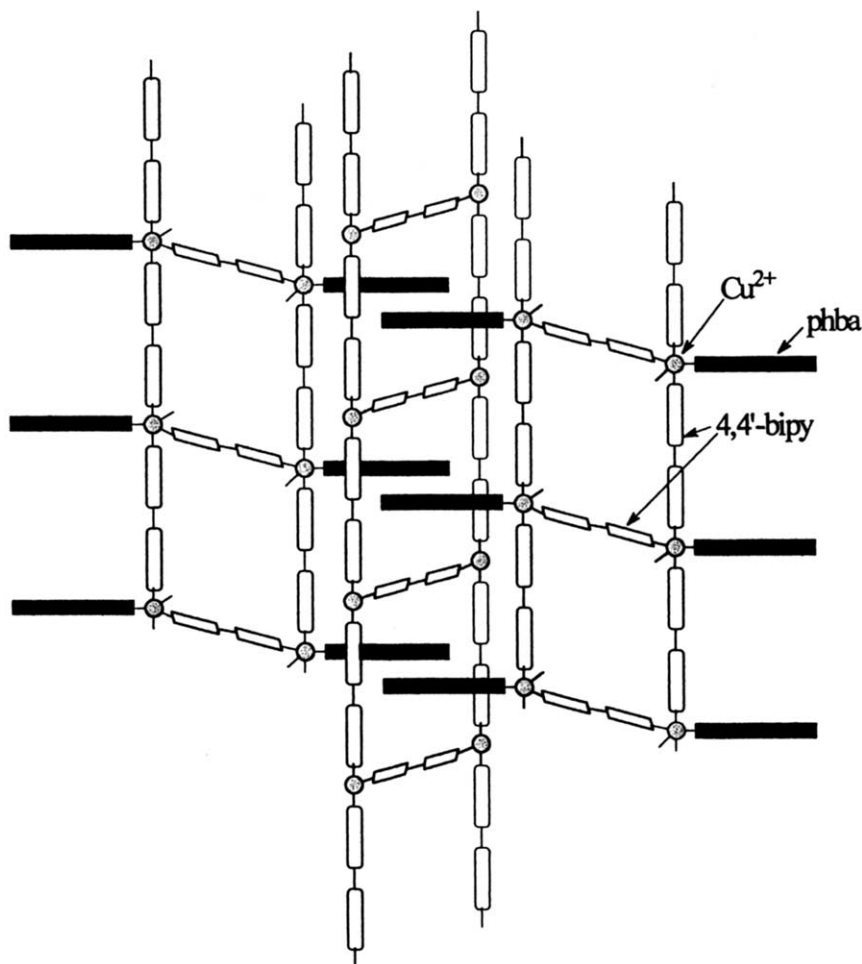
penetrate into the same square, are parallel to each other and to those of 4,4'-bipy. The face-to-face separation between the aromatic rings of phba arms is about 3.49 Å, while the face-to-face separation between the phba ring and 4,4'-bipy is in the range 3.36–3.59 Å, indicating, in both cases, significant  $\pi$ - $\pi$  interactions.

A particular case is that of the lanthanide(III)–4,4'-bipy systems. The following series of compounds have been characterized:

$(4,4'\text{-Hbipy})[\text{Ln}(\text{NO}_3)_4(\text{H}_2\text{O})_2(4,4'\text{-bipy})]$ , Ln = La, Ce, Pr, Nd [37];  $[\text{Ln}(\text{NO}_3)_3(\text{H}_2\text{O})_n] \cdot 2(4,4'\text{-bipy}) \cdot \text{H}_2\text{O}$ , Ln = La ( $n = 3$ ); Nd ( $n = 4$ ), Pr ( $n = 4$ ) [38];  $[\text{Ln}(\text{NO}_3)_3(\text{H}_2\text{O})_3] \cdot 2(4,4'\text{-bipy})$ , Ln = Y, Sm, Eu, Gd, Tb, Dy, Ho [39];  $[\text{Ln}_2(\text{NO}_3)_6(\text{H}_2\text{O})_7] \cdot 4(4,4'\text{-bipy})$  Ln = La, Ce, Pr [39].

In the first series, 4,4'-bipy acts as a monodentate ligand, while in the others it is uncoordinated.

Two binuclear complexes with 4,4'-bipy bridges between Ln(III) ions are known so far:  $(4,4'\text{-Hbipy})_2[\text{Nd}_2(4,4'\text{-bipy})(\text{NO}_3)_8(\text{H}_2\text{O})_4] \cdot 3(4,4'\text{-bipy})$  [40] and  $[\text{Lu}_2\text{L}_6(4,4'\text{-bipy})]$  (L = dimethyl-*N*-trichloroacetylaminodiphosphate anion) [41]. In one case, namely in a



Scheme 15.

Tb(III) compound,  $[\text{Tb}_2(\text{O}_2\text{CPh})_6(4,4'\text{-bipy})]$ , the 4,4'-bipy bridging molecules propagate extended structures [42].

The compounds belonging to the first two series crystallize in the chiral space group  $P2_12_12_1$  and, therefore, are particularly interesting in crystal engineering. They show that lanthanides are suited to induce dissymmetry by coordination with appropriate ligands, resulting in chiral extended networks. In the first family of compounds,  $(4,4'\text{-Hbipy})[\text{Ln}(\text{NO}_3)_4(\text{H}_2\text{O})_2(4,4'\text{-bipy})]$ , chiral open 3-D grids are formed through hydrogen bond interactions between the complex anions,  $[\text{Ln}(\text{NO}_3)_4(\text{H}_2\text{O})_2(4,4'\text{-bipy})]^-$ , and the organic cations,  $[4,4'\text{-Hbipy}]^+$  (Fig. 7). Two independent networks interpenetrate.

In the second family, the  $[\text{Ln}(\text{NO}_3)_3(\text{H}_2\text{O})_n]$  mononuclear species form layered hydrogen bonded structures, which are interconnected by 4,4'-bipy pillars.

The nature of the compounds resulted from the interaction of the lanthanides(III) ions with bis(4-pyridyl) ligands was found to be very sensitive to the pH of the solutions.

An alternative way toward chiral networks is the self-assembly of preformed chiral coordination motifs with 4,4'-bipy spacers. Several interesting examples are found again in the chemistry of lanthanides [43]. The reaction between lanthanide perchlorates and the tripodal ligand tris(2-benzimidazolyl)amine (ntb) gives chiral  $[\text{Ln}(\text{ntb})_2]^{3+}$  cations. The Ln(III) ions are eight-coordinated and display a slightly distorted cubic environment (it is noteworthy that this stereochemistry is quite rare for the coordination number of eight). Each ntb ligand possesses three NH groups that are potential hydrogen bond donors. These can be exploited by assembling the  $[\text{Ln}(\text{ntb})_2]^{3+}$  moieties with linear difunctional hydrogen bond acceptors, for example 4,4'-bipy. Indeed, the cocrystallization process of the Ln(III) complexes with linear spacers (4,4'-bipy, *trans*-1,2-bis(4-pyridyl)ethylene (bpete) leads to 3-D networks sustained by hydrogen bond interactions:

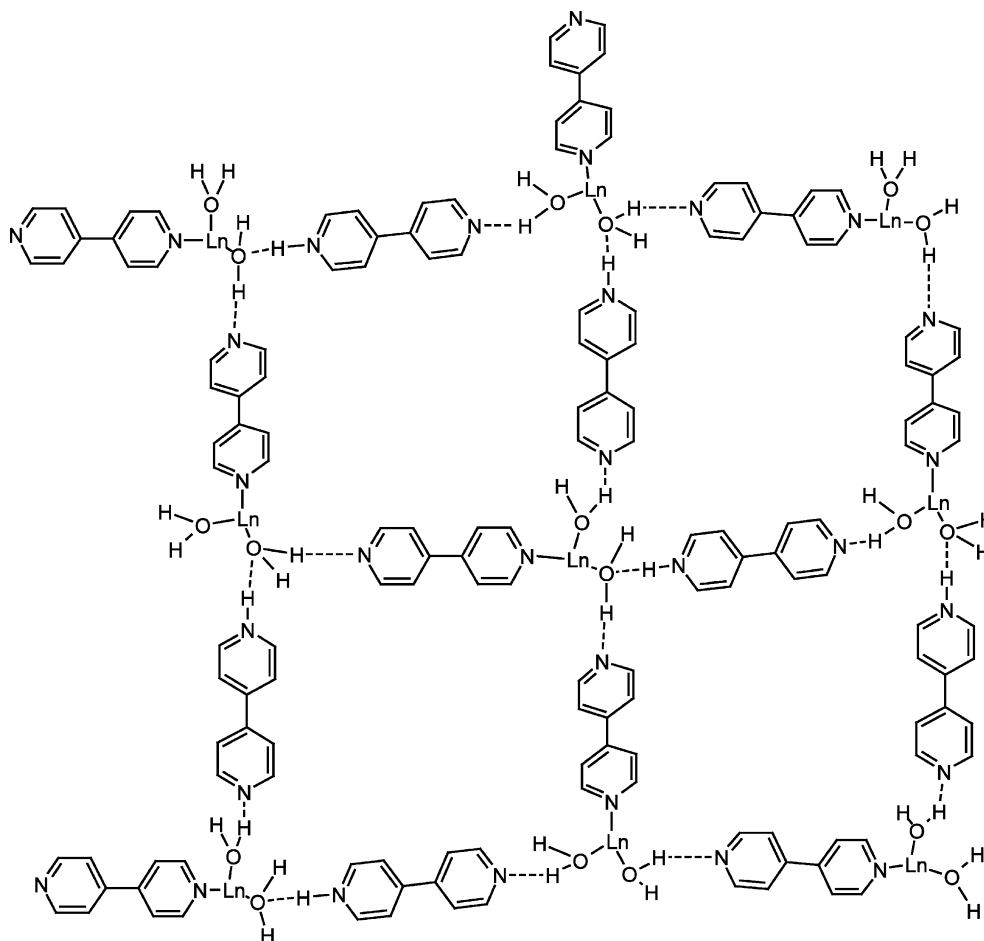
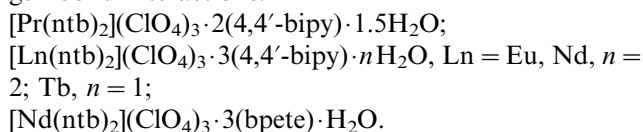
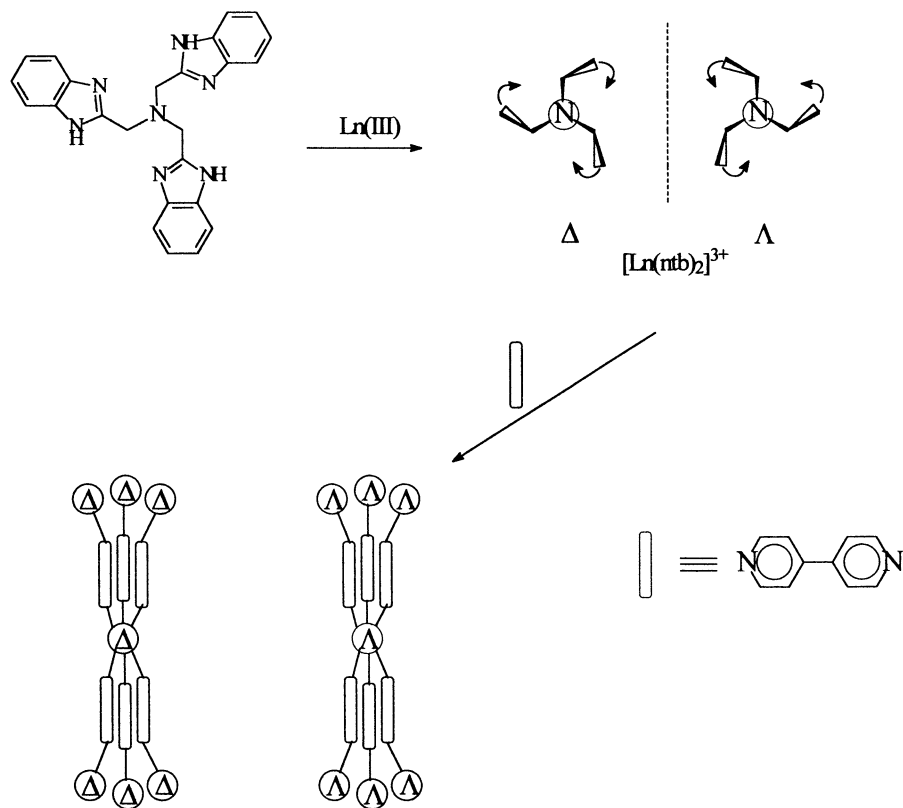


Fig. 7. Open framework resulted from hydrogen bonds between  $[\text{La}(\text{NO}_3)_4(\text{OH}_2)_2(4,4'\text{-bipy})]^-$  ions and  $[4,4'\text{-Hbipy}]^+$ . The nitrate groups are not represented (adapted from Ref. [38a]).



Scheme 16.

The Eu(III), Nd(III) and Tb(III) derivatives,  $[\text{Ln}(\text{ntb})_2](\text{ClO}_4)_3 \cdot 3(4,4'\text{-bipy}) \cdot n\text{H}_2\text{O}$  are particularly interesting. Two ntb ligands are coordinated to the Ln(III) ions in such a way that a  $C_3$  axis passes through the two apical tertiary amino nitrogen atoms and the metal ion. Viewing down the  $C_3$  axis, the two ntb ligands have the same right- or left-handed propeller configuration. This helical arrangement results in pairs of  $\Delta$  and  $\Lambda$  enantiomers. The complex cation,  $[\text{Ln}(\text{ntb})_2]^{3+}$ , has six NH groups arising from the two ntb ligands. All these groups interact with six linear difunctional hydrogen

bond acceptors (4,4'-bipy) (Fig. 8). The spacers promote the aggregation of isomers of the same chirality, resulting in an extended 3-D network (Fig. 9) designed as  $\Delta_3\text{-}\Delta \dots$  or  $\Lambda_3\text{-}\Lambda \dots$  (Scheme 16). Two networks of the same handedness interpenetrate to form a chiral framework. In  $[\text{Nd}(\text{ntb})_2](\text{ClO}_4)_3 \cdot 3(\text{bpete}) \cdot \text{H}_2\text{O}$ , the other spacer, bpete, connects either a pair of enantiomers, or the same chiral  $[\text{Nd}(\text{ntb})_2]^{3+}$  cations, generating a 3-D racemic compound. The enantioselective self-assembly in the case of the 4,4'-bipy derivative has been explained by the possibility of the pyridyl rings in 4,4'-

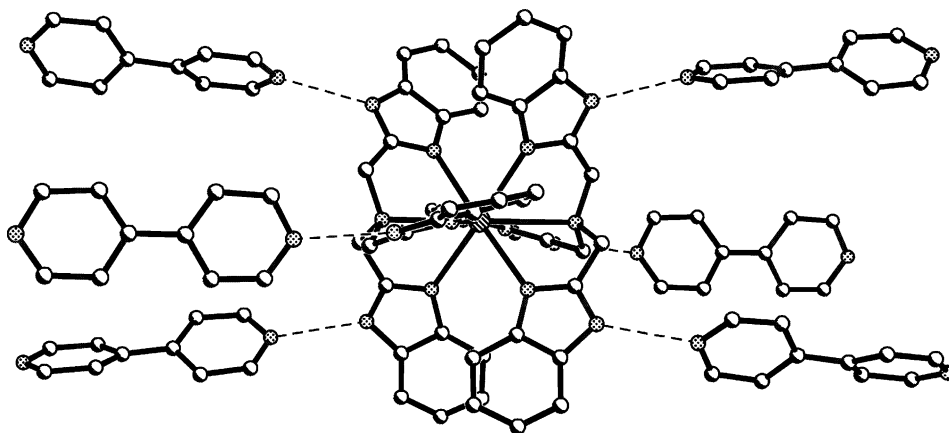


Fig. 8. Hydrogen bond interactions between the six NH groups arising from the two ntb ligands in  $[\text{Nd}(\text{ntb})_2](\text{ClO}_4)_3 \cdot 3(4,4'\text{-bipy}) \cdot 2\text{H}_2\text{O}$  and six 4,4'-bipy spacers (adapted from Ref. [43b]).

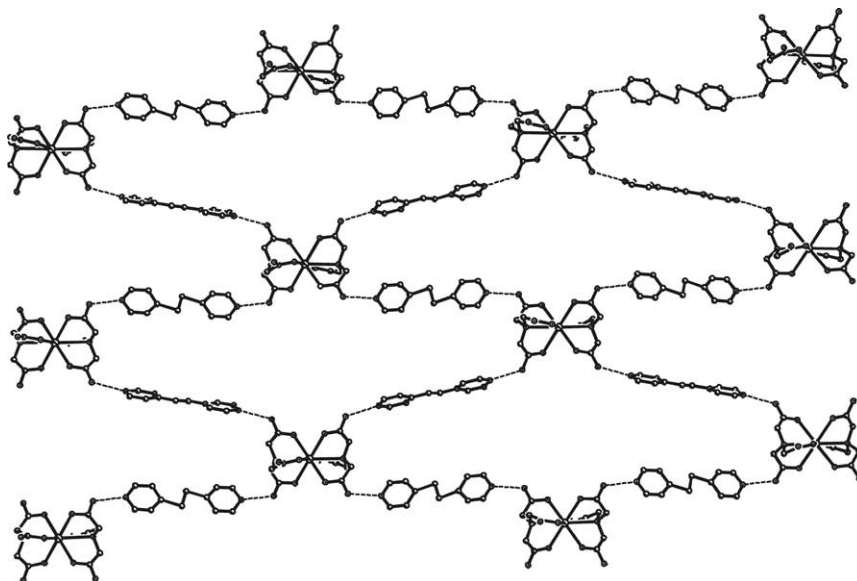


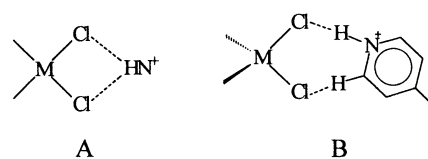
Fig. 9. View of one independent network in  $[\text{Nd}(\text{ntb})_2](\text{ClO}_4)_3 \cdot 3(4,4'\text{-bipy}) \cdot 2\text{H}_2\text{O}$  (adapted from Ref. [43b]).

bipy to rotate freely, while the ethylene double bond in bpete imposes a coplanar conformation. The pyridyl moieties in  $[\text{Nd}(\text{ntb})_2](\text{ClO}_4)_3 \cdot 3(4,4'\text{-bipy}) \cdot 2\text{H}_2\text{O}$  are rotated with a dihedral angle of ca.  $31^\circ$ , which seems to favor the connection of neighboring  $[\text{Nd}(\text{ntb})_2]^{3+}$  cations of the same chirality.

#### 4. The $[4,4'\text{-H}_2\text{bipy}]^{2+}$ tecton: organic–inorganic hybrid materials constructed from $\text{MX} \cdots \text{HN}^+$ synthons

The diprotonated 4,4'-bipy, that is, the  $[4,4'\text{-H}_2\text{bipy}]^{2+}$  cation, can generate interesting solid-state architectures through hydrogen bond interactions with  $[\text{MX}_4]^{2-}$  anions. A whole family of crystalline salts of the type  $[4,4'\text{-H}_2\text{bipy}][\text{MX}_4]$  has been characterized:  $\text{X} = \text{Cl}$ ,  $\text{M} = \text{Pd}$ ,  $\text{Pt}$ ,  $\text{Co}$ ,  $\text{Zn}$ ,  $\text{Hg}$ ,  $\text{Mn}$ ,  $\text{Cd}$ ,  $\text{Pb}$ ;  $\text{X} = \text{Br}$ ,  $\text{M} = \text{Pd}$ ,  $\text{Co}$ ,  $\text{Zn}$ ,  $\text{Mn}$  [44];  $\text{X} = \text{NCS}$ ,  $\text{M} = \text{Mn}$ ,  $\text{Co}$ ,  $\text{Zn}$  [45].

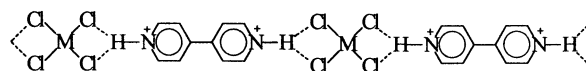
In the perhalometallate series, the solid-state architectures are built up from the supramolecular synthons **A** and **B** (Scheme 17). The synthon **A** is present in 1-D chains constructed from two building blocks: square-planar  $[\text{MCl}_4]^{2-}$  ( $\text{M} = \text{Pd}$ ,  $\text{Pt}$ ) and  $[4,4'\text{-H}_2\text{bipy}]^{2+}$  ions (Scheme 18). The resulting ribbons are planar and parallel. If the metal ion prefers another coordination geometry, for instance a tetrahedral one ( $\text{M} = \text{Co}$ ,  $\text{Zn}$ ,  $\text{Hg}$ ), dimeric cyclic motifs, constructed from synthon **B**, are formed (Scheme 19). The difference between the structures generated by the mononuclear  $[\text{MCl}_4]^{2-}$  anions (Schemes 18 and 19) can be rationalized by observing that the increased  $\text{Cl-M-Cl}$  angle in the tetrahedral geometry prevents the formation of synthon **A**. For  $\text{M} = \text{Mn}$ ,  $\text{Cd}$ ,  $\text{Pb}$ , another structural motif results: these systems contain  $[\text{MCl}_6]$  octahedral units,



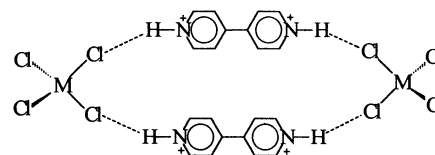
Scheme 17.

linked by *cis* edge-sharing infinite  $[\{\text{MX}_4\}_n]^{2n-}$  chains. These chains are further cross-linked by hydrogen bonded  $[4,4'\text{-H}_2\text{bipy}]^{2+}$ , forming neutral sheets. The structure of the  $\text{Pb}(\text{II})$  derivative is presented in Scheme 20: the infinite chains are linked by synthon **A**. This interaction involves two terminal chloride at one end of the  $[4,4'\text{-H}_2\text{bipy}]^{2+}$  cation, and two bridging chlorides at the other one. These examples nicely illustrate the important role played by the coordination geometry of the metal ions in determining the solid-state architectures of compounds with identical stoichiometry and non-intervening solvent molecules.

Three isostructural compounds have been characterized in the  $[4,4'\text{-H}_2\text{bipy}][\text{M}(\text{NCS})_4]$  family:  $\text{M} = \text{Mn}$ ,  $\text{Co}$ ,

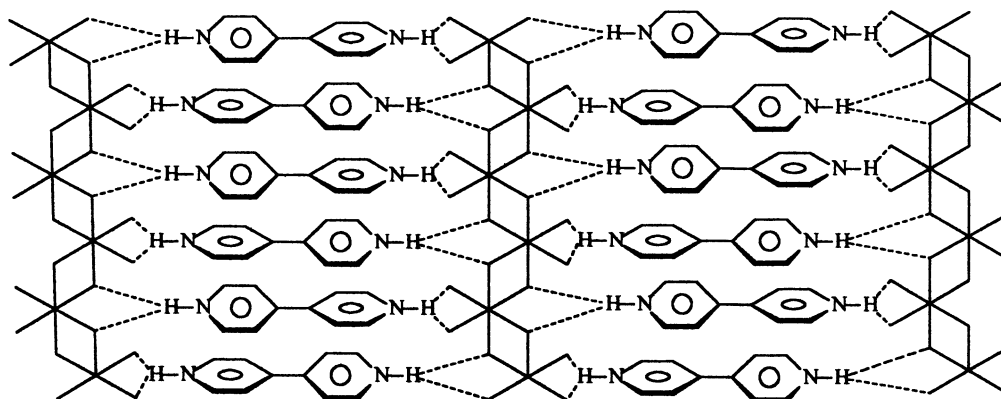


Scheme 18.



Scheme 19.





Scheme 20.

Zn. All of them crystallize in the chiral orthorhombic space group  $P2_12_12$  and have particular relevance in materials science, namely materials exhibiting non-linear optical properties. The solid-state architecture results from an interesting convolution of two types of non-covalent interactions. The  $[\text{M}(\text{NCS})_4]^{2-}$  anions interact through weak  $\text{S} \cdots \text{S}$  contacts (the distances associated

with these contacts range from 3.63 to 3.64 Å in all three compounds). Two-dimensional networks are formed (Fig. 10). These networks are stacked with each other, generating channels, in which the  $[\text{4,4'}\text{-H}_2\text{bipy}]^{2+}$  cations are accommodated (the hydrogen bonds are established with the sulfur atoms). The  $[\text{M}(\text{NCS})_4]^{2-}$  anions and the  $[\text{4,4'}\text{-H}_2\text{bipy}]^{2+}$  cations are arranged into

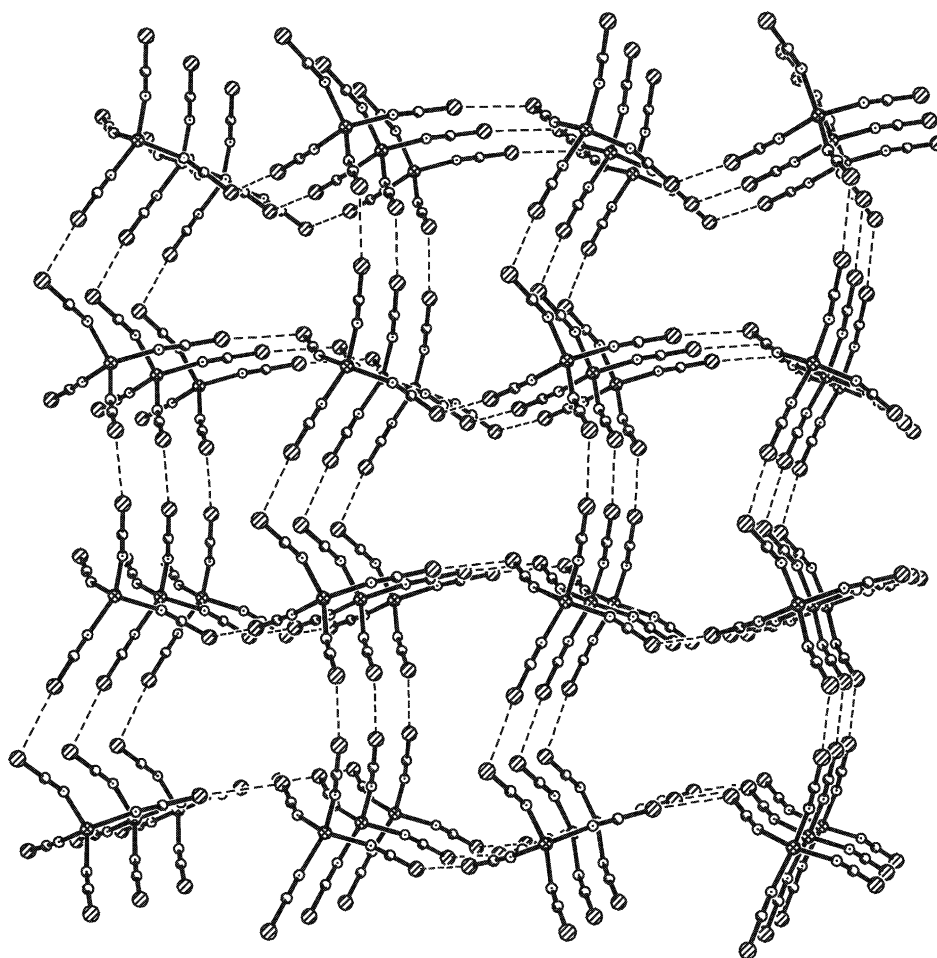


Fig. 10. Layers resulting from  $\text{S} \cdots \text{S}$  contacts between the  $[\text{M}(\text{NCS})_4]^{2-}$  ions in compounds  $[\text{4,4'}\text{-H}_2\text{bipy}][\text{M}(\text{NCS})_4]$  (adapted from Ref. [45]).

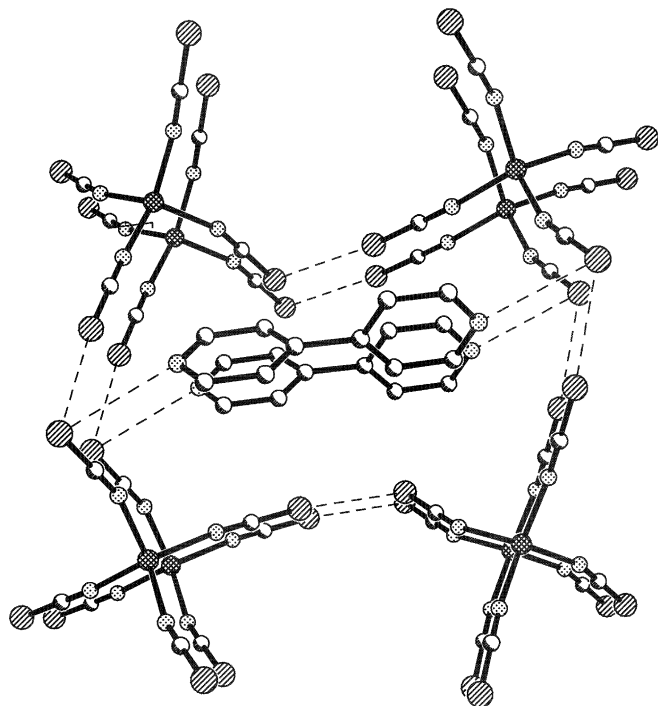
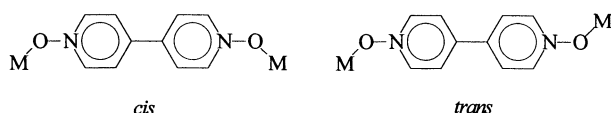


Fig. 11. Hydrogen bond interactions between  $[4,4'\text{-H}_2\text{bipy}]^{2+}$  and  $[\text{M}(\text{NCS})_4]^{2-}$  anions in compounds  $[4,4'\text{-H}_2\text{bipy}][\text{M}(\text{NCS})_4]$  (adapted from Ref. [45]).

a 2-D, wavy network (Fig. 11). The zinc derivative is NLO active, and has a moderate second harmonic generation efficiency (0.21 times that of urea).

### 5. 4,4'-Bipyridine-*N,N'*-dioxide—a new tecton in crystal engineering

In contrast with 4,4'-bipy, the potentialities of 4,4'-bipyridine-*N,N'*-dioxide (4,4'-bpno) in crystal engineering and in the construction of coordination networks have been only little exploited. 4,4'-Bpno is a rigid spacer, like the related 4,4'-bipy molecule, and can act both as a bridging or terminal ligand. Its aromatic rings can be involved also in  $\pi$ - $\pi$  aromatic interactions. On the other hand, 4,4'-bpno has several peculiarities: (a) it can form bridges with different geometries (*cis* and *trans* coordination modes—Scheme 21); (b) it is a better hydrogen acceptor than 4,4'-bipy; (c) due to the orientation of the lone pairs at the oxygen atoms, it presents a rich variety of connectivity modes through hydrogen bond interactions, which are summarized in Scheme 22.



Scheme 21.

The metal-(4,4'-bpno) molar ratio of 1:1 leads, as expected, to chains (Scheme 23) [46]. The distance between the bridged metal ions is larger than in the 4,4'-bipy analogues. Fig. 12 shows such a chain resulted from the reaction of a heteropolynuclear complex,  $[\text{Mn}\{\text{Cr}(\text{bipy})(\text{C}_2\text{O}_4)_2\}_2]$ , with 4,4'-bpno [46b].

As in the case of 4,4'-bipy, the increasing amount of the *exo*-bidentate molecules leads to interesting 2- or 3-D frameworks. For d-block elements, only a few compounds have been synthesized so far:

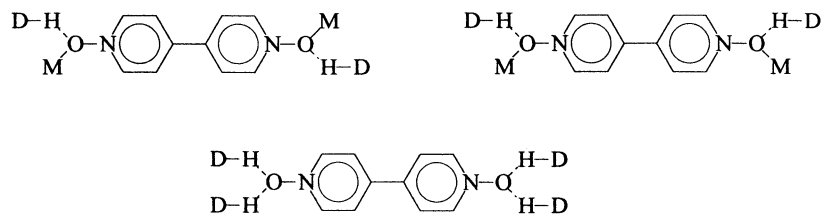
$[\text{M}(4,4'\text{-bpno})(\text{H}_2\text{O})_4](\text{ClO}_4)_2 \cdot 2(4,4'\text{-bpno})$  ( $\text{M} = \text{Co}$ , **23**,  $\text{M} = \text{Ni}$ , **24**,  $\text{M} = \text{Cu}$ , **25**,  $\text{M} = \text{Zn}$ , **26**) [47];

$[\text{Zn}(\text{MeOH})_3(4,4'\text{-bpno})_3]\text{SiF}_6 \cdot 3\text{MeOH}$  (**27**) [48];

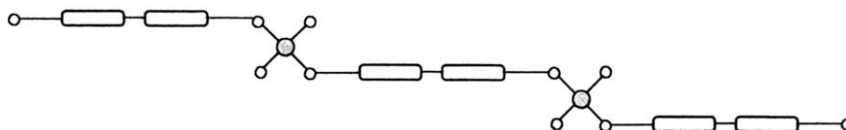
$[\text{Zn}(4,4'\text{-bpno})_6](\text{NO}_3)_2$  (**28**) [48].

Compounds **23–26** are isostructural and isomorphous (triclinic,  $P\bar{1}$ ). One 4,4'-bpno molecule acts as a bridging ligand, forming a 1-D coordination polymer of the type presented in Scheme 23. The metal ions ( $\text{Co}(\text{II})$ ,  $\text{Ni}(\text{II})$ ,  $\text{Cu}(\text{II})$  or  $\text{Zn}(\text{II})$ ) are octahedrally coordinated by four aqua ligands and two oxygen atoms arising from the *trans*-coordinated 4,4'-bpno bridging ligands. In compound **25**, the  $\text{Cu}(\text{II})$  ion exhibits a significant tetragonal distortion, due to the manifestation of the Jahn–Teller effect: four short bonds with the aqua ligands (average 1.96 Å), and two long bonds with the oxygen atoms arising from the bridging ligands (2.407 Å). The 3-D order in the crystal is achieved through hydrogen bond interactions involving both coordinated and uncoordinated 4,4'-bpno molecules. Adjacent chains are connected through hydrogen bonds established between the bridging 4,4'-bpno ligands and the aqua ligands from neighboring chains (Scheme 24), leading to a 2-D structural motif in the [110] plane (Fig. 13). The uncoordinated 4,4'-bpno molecules play a special role in increasing the dimensionality of the supramolecular architecture. The 3-D structure can be viewed as resulting from interweaving two sets of sheets. One set is that illustrated in Fig. 13, while the other is generated in the plane [111] by half of the uncoordinated 4,4'-bpno molecules, through hydrogen bonds with the aqua ligands (Fig. 14). These sheets are further connected by the other half of uncoordinated 4,4'-bpno molecules, which are also hydrogen bonded to the aqua ligands, yielding triangular channels hosting the perchlorate anions (Fig. 15).

In compound **27**, the 4,4'-bpno molecules exhibit different functions: bridging, terminal and uncoordinated (Scheme 25). Each zinc atom is hexacoordinated by four oxygen atoms arising from four different N-oxide ligands and two oxygen atoms from the coordinated methanol molecules. At each zinc ion, one 4,4'-bpno molecule acts as a terminal ligand and is involved in hydrogen bond interactions with the methanol molecule coordinated to another zinc ion. The uncoordinated N-oxide molecule is hydrogen bonded to two



Scheme 22.



Scheme 23.

methanol molecules coordinated to different zinc ions (Scheme 25). The bridging 4,4'-bpno ligands generate a 2-D brick wall layer. The uncoordinated N-oxide molecules join through hydrogen bonds the nodes at centers of the long side of the rectangles, resulting in a square network topology (Fig. 16). The terminal N-oxide ligands expand the structure in the third dimension through hydrogen bond interactions with the methanol molecules of another sheet, resulting in an open network with large channels ( $10.2 \times 14.2 \text{ \AA}$ ), which are occupied by the solvent molecules and the anions.

In compound **28**, all six 4,4'-bpno molecules are terminal ligands, the complex being mononuclear. The reduced steric requirements of 4,4'-bpno, in comparison with 4,4'-bipy, allow the coordination of six ligands around the metal ion. This is not possible in the case of 4,4'-bipy ligand. The supramolecular architecture of **28** results from face-to-face  $\pi$ - $\pi$  intermolecular interactions ( $3.27$ – $3.39 \text{ \AA}$ ) involving each terminal N-oxide ligand, which give 2-D sheets (Fig. 17). The formation of compound **28** is independent of the starting metal-to-ligand molar ratio (it is obtained even by working with

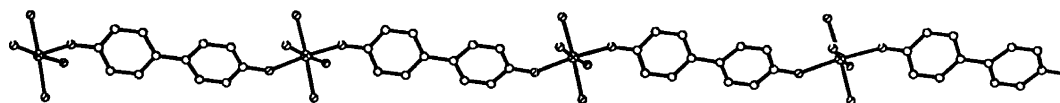


Fig. 12.  $\{[\text{Mn}(\text{H}_2\text{O})_4(4,4'\text{-bpno})]\}^{2n+}$  zigzag chains in compound  $[\text{Mn}(\text{H}_2\text{O})_4(4,4'\text{-bpno})][\text{Cr}(\text{bipy})(\text{C}_2\text{O}_4)_2] \cdot 8\text{H}_2\text{O}$  [29]. Within the chains, the distance between the Mn(II) ions is  $13.248 \text{ \AA}$ .

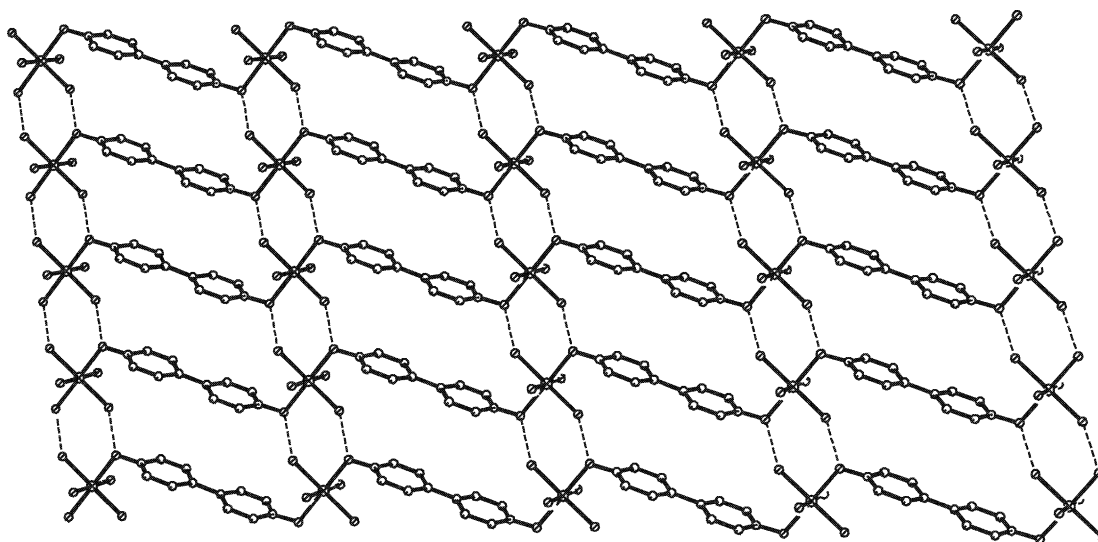
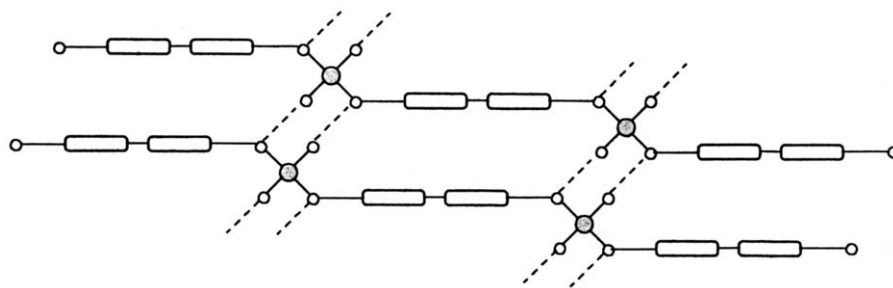
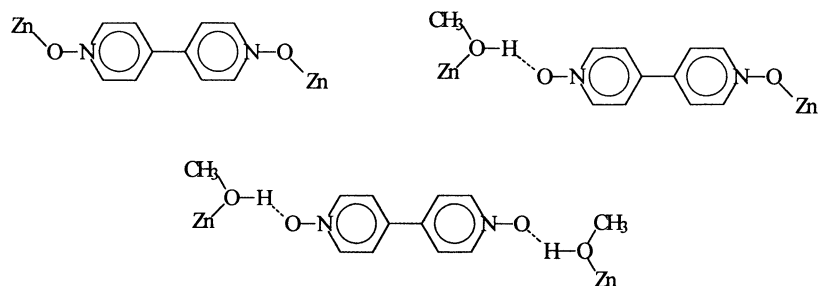


Fig. 13. Two-dimensional sheet in compounds **23**–**26** resulted through hydrogen bonding between bridging 4,4'-bpno and aqua ligands in the  $[110]$  plane (adapted from Ref. [47a]).



Scheme 24.



Scheme 25.

1:2 molar ratio). Although compounds **27** and **28** are obtained under similar conditions, their structures are very different, suggesting a key templating role of the anions.

A particularly interesting solid-state supramolecular architecture is observed with the tetranuclear Cu(II)

complex  $[\{L(\mu\text{-OH})\text{Cu}_2\}-(\mu\text{-4,4'-bpno})-\{L(\mu\text{-OH})\text{Cu}_2\}-(\text{ClO}_4)_4]$  (**29**) [49]. Compound **29** has been obtained by reacting a binuclear precursor,  $[\text{L}(\mu\text{-OH})\text{Cu}_2](\text{ClO}_4)_2$ , with 4,4'-bpno. L is a compartmental end-off ligand, 2,6-bis[*N*-(2-pyridylethyl)formimidoyl]-4-methyl-phenolato, which is obtained from the reaction of 2,6-

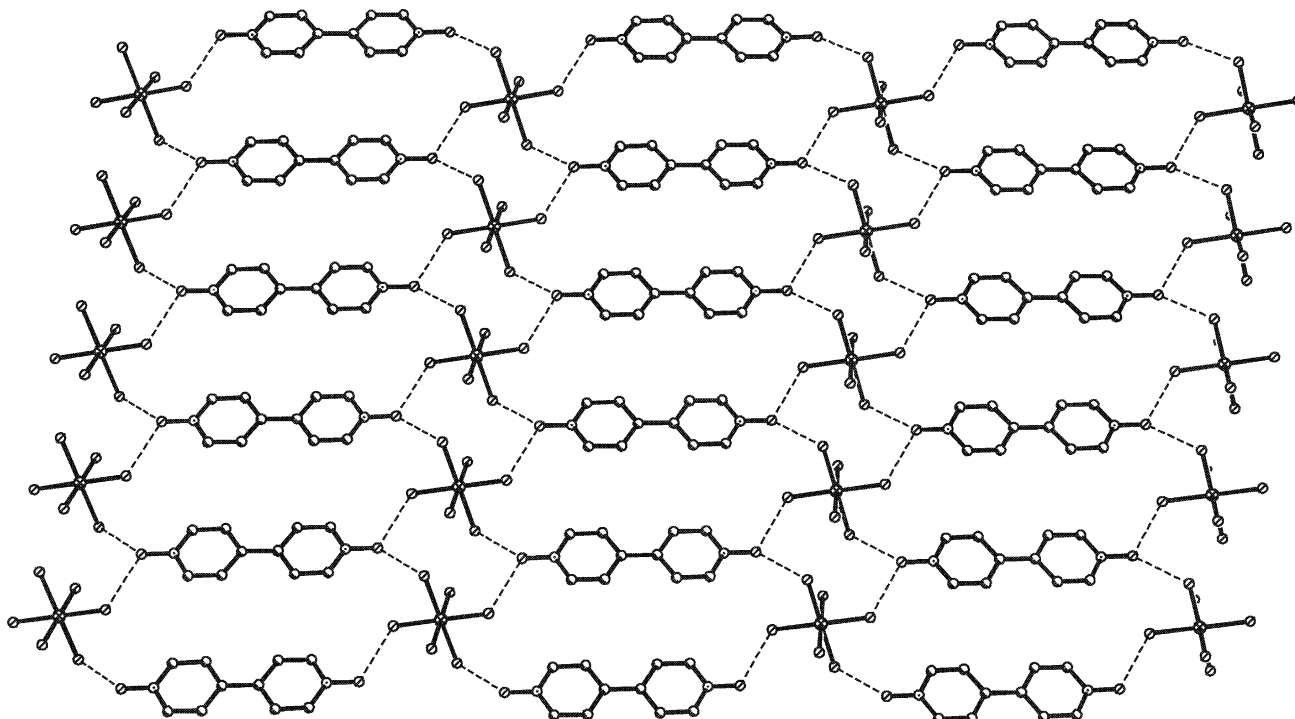


Fig. 14. Two-dimensional layer in compounds **23–26** resulted from hydrogen bond interactions between uncoordinated 4,4'-bpno molecules and the aqua ligands in the [111] plane (adapted from Ref. [47a]).

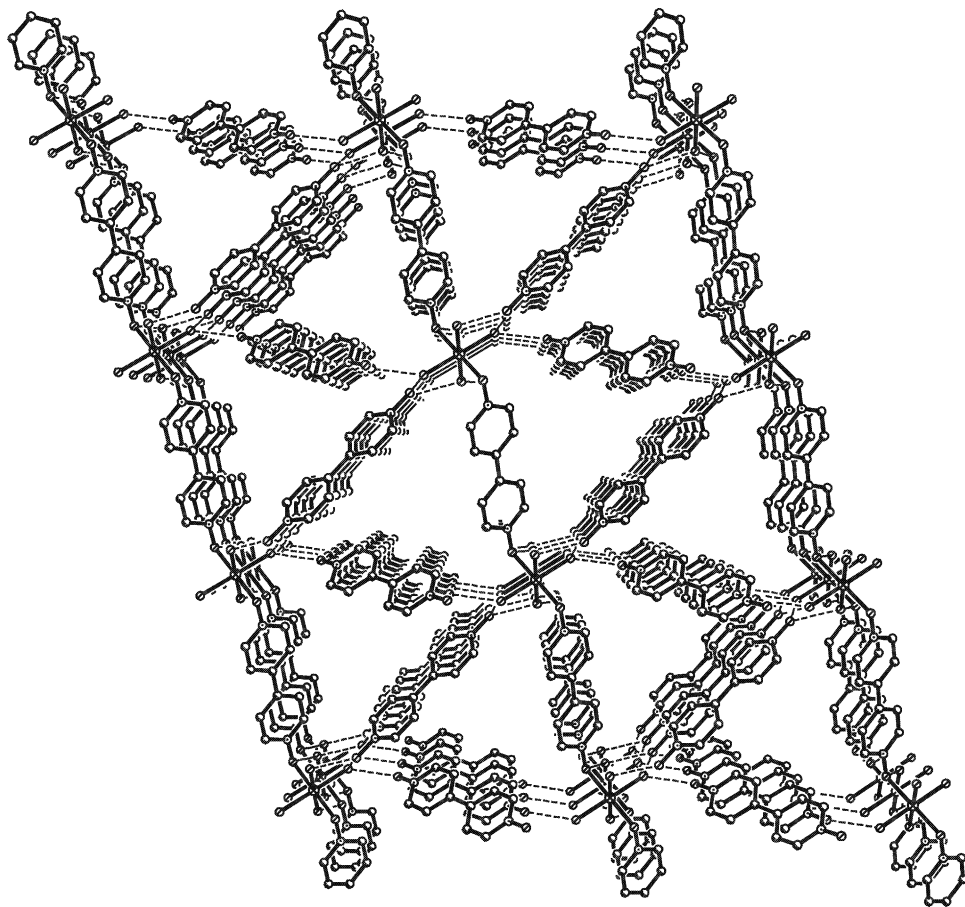


Fig. 15. The 3-D network in compounds **23–26** (adapted from Ref. [47a]).

diformyl-4-methyl-phenol with 2-(2-aminoethyl)pyridine. The starting binuclear complex contains the

$\text{HO}^-$  ion acting as an exogenous bridge. In **29**, one 4,4'-bpno molecule bridges two Cu(II) ions arising from

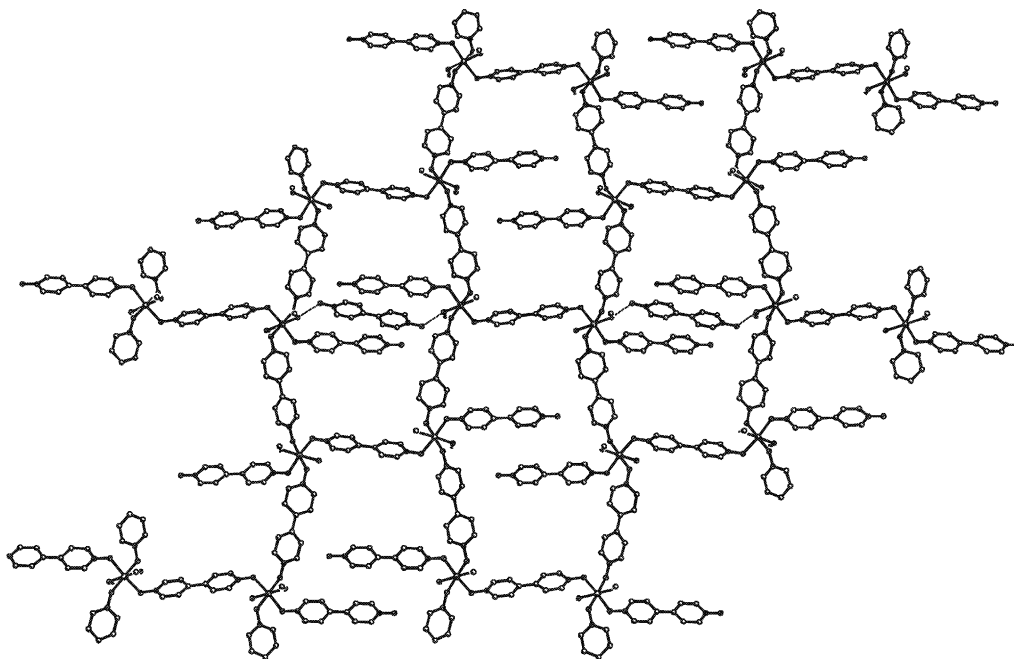


Fig. 16. View of a sheet in compound **27** (adapted from Ref. [48]).



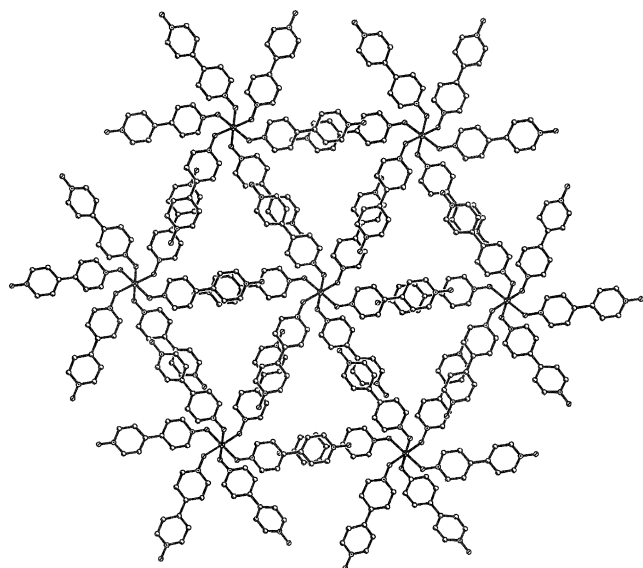


Fig. 17. View of the layer structure of compound **28**, resulted from  $\pi$ – $\pi$  stacking interactions (adapted from Ref. [48]).

two binuclear entities (Fig. 18). The other two Cu(II) ions, which are not bridged by 4,4'-bpno, exhibit a square-planar stereochemistry. Two *trans* lone pairs

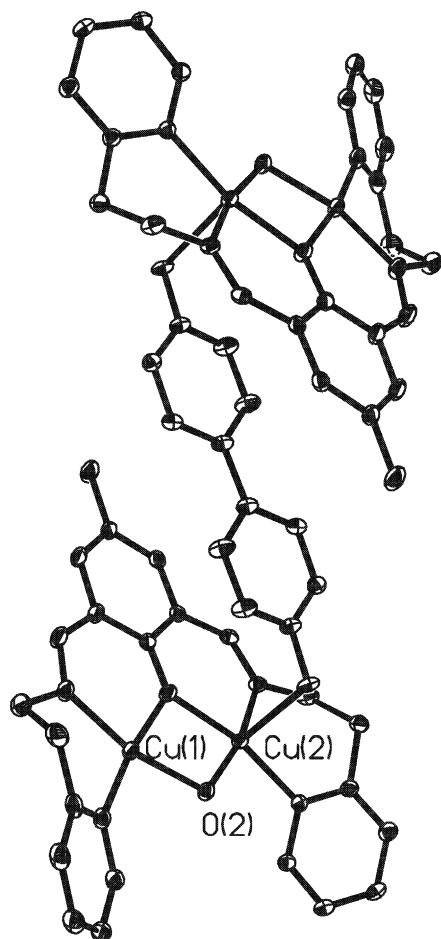


Fig. 18. Molecular structure of the tetranuclear Cu(II) complex **29**.

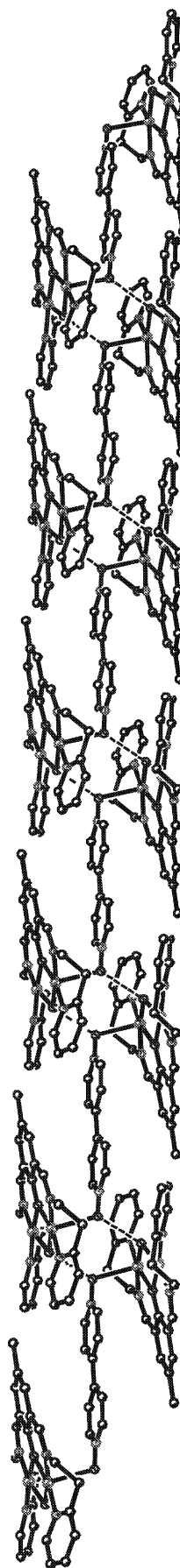


Fig. 19. Packing diagram of compound **29**, showing the hydrogen bonded polymer.

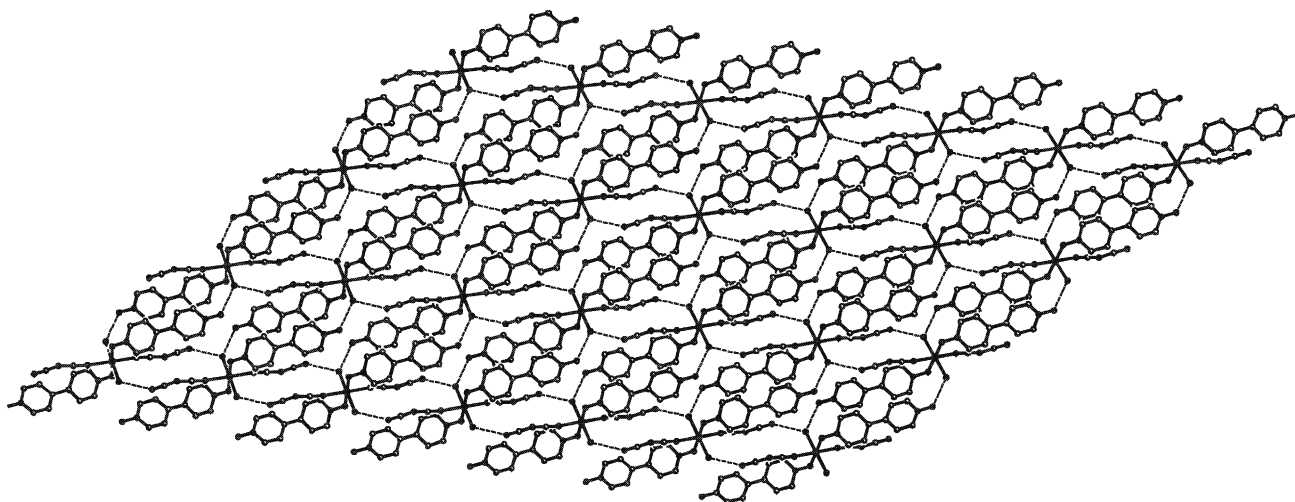


Fig. 20. Two-dimensional network in compound **30** [50].

from the oxygen atoms of 4,4'-bpno are involved in hydrogen bond interactions with the bridging  $\text{HO}^-$  groups from neighboring tetranuclear entities ( $\text{O} \cdots \text{H} \cdots \text{O} = 2.76 \text{ \AA}$ ), resulting in a hydrogen bonded polymer with a unique topology, that is, a hydrogen bonded polymer having a tetranuclear repeating unit (Fig. 19).

By reacting Co(II) or Mn(II) perchlorate with  $\text{Na}[\text{N}(\text{CN})_2]$  and 4,4'-bpno, isomorphous complexes of formula  $[\text{M}(4,4'\text{-bpno})_2\{\text{N}(\text{CN})_2\}_2(\text{H}_2\text{O})_2]$  (**30**) are obtained. The 4,4'-bpno molecules act here as terminal ligands, hydrogen bond interactions between the 4,4'-bpno, the dicyanamido and the aqua ligands generate a 2-D network—Fig. 20 [50].

Since the lanthanide ions are hard acids and extremely oxophilic, pyridine-*N*-oxides are expected to be very good ligands for them. Coordination networks with lanthanide, as nodes, and 4,4'-bpno molecules, as spacers, have been only very recently reported, and show a rich structural diversity [51]. The compounds reported till now [51] do not show hydrogen bond or  $\pi$ - $\pi$  stacking interactions playing a structural role in the overall architecture of the crystal.

The topologies of the networks containing lanthanides and 4,4'-bpno as a spacer are much more difficult to be controlled than those containing 3d metal ions: lanthanides have flexible coordination spheres, with various coordination numbers and geometries.

By combining the bridging ability 4,4'-bpno with the well known one of the cyano groups, it was possible to design 3d–4f heterometallic coordination polymers with novel supramolecular architectures. A family of isomorphous and isostructural compounds has been obtained by reacting aqueous solutions of  $\text{Pr}(\text{NO}_3)_3$  and  $\text{K}_3[\text{M}(\text{CN})_6]$  ( $\text{M} = \text{Cr}(\text{III}), \text{Co}(\text{III}), \text{Fe}(\text{III})$ ) with an alcoholic solution of 4,4'-bpno:  $[\{(\text{H}_2\text{O})_5(4,4'$ -

bpno) $\text{Pr}-\text{NC}-\text{M}(\text{CN})_5\}(\mu\text{-}4,4'\text{-bpno})] \cdot 0.5(4,4'\text{-bpno}) \cdot 4\text{H}_2\text{O}$  (**31**) [52]. Their 3-D architecture is based on the convolution of coordinative with hydrogen bonding and  $\pi$ - $\pi$  interactions. The structure can be described as being formed by  $\{(\text{H}_2\text{O})_5\text{LPr}-\text{NC}-\text{Fe}(\text{CN})_5\}$  neutral binuclear entities, which are bridged by 4,4'-bpno, resulting in infinite zigzag chains (Fig. 21). Within the binuclear moieties, the  $[\text{M}(\text{CN})_6]^{3-}$  anion acts as a monodentate ligand, that is, with one  $\text{CN}^-$  group coordinated to the praseodymium atom. Three 4,4'-bpno molecules are directly bonded to one Pr(III) ion. Two of them form bridges between the praseodymium atoms, while the third one acts as a terminal ligand. The Pr(III) ion exhibits a co-ordination number of nine: eight oxygen atoms, arising from five aqua and three L ligands, and one nitrogen atom from the cyano bridge. The Pr(III) ions are alternatively 'bridged' through intrachain hydrogen bonds involving uncoordinated 4,4'-bpno molecules and the aqua ligands. The distance between the triply 'bridged' praseodymium atoms ( $13.43 \text{ \AA}$ ) is slightly shorter than the one between the simply bridged atoms ( $13.93 \text{ \AA}$ ).

The terminal organic ligands further extend the structure through  $\pi$ - $\pi$  stacking with identical terminal L ligands from adjacent zigzag chains, resulting in brick wall-like sheets (Fig. 22). The distances for the ligand-to-ligand  $\pi$ - $\pi$  interactions are in the range  $3.47$ – $3.51 \text{ \AA}$ . The perfect face-to-face  $\pi$ -stacked alignment of the peripheral pyridyl-*N*-oxide moieties of the terminal ligands is clearly favored by dipole-dipole interactions (Scheme 26). The uncoordinated 4,4'-bpno molecules play a special role in increasing the dimensionality of the supramolecular architecture. Each uncoordinated molecule is simultaneously hydrogen bonded to four aqua ligands, two of these being coordinated to two adjacent Pr(III) ions in a chain, while the other two aqua ligands

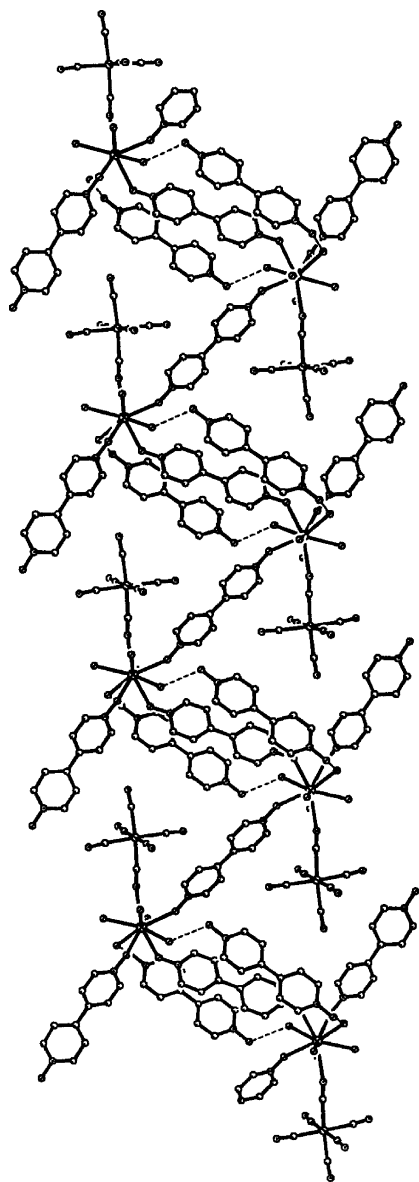
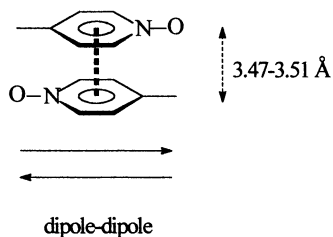


Fig. 21. Perspective view of a zigzag chain in compounds **31** also showing the uncoordinated 4,4'-bipyridine-*N,N'*-dioxide molecules, which are hydrogen bonded to the aqua ligands coordinated to the Pr(III) ions (adapted from Ref. [52]).

arise from another chain belonging to a neighboring brick wall sheet (Fig. 23). Since the Ln(III)–NC–M(CN)<sub>5</sub> units are well separated in the crystal, such



Scheme 26.

compounds are suited for the study of the magnetic interactions between Ln(III) ions and Cr(III) or Fe(III).

At this stage, the supramolecular architectures, constructed by simultaneous use of hexacyanometalate and 4,4'-bpno building-blocks, are quite unusual and difficult to be rationalized. The way from serendipitous to rational level in designing such networks is still long. On the other hand, the resulting topologies of the spin carriers in 3d–4f coordination networks is of current interest in molecular magnetism and open new perspectives to magneto-structural correlation.

The new coming building-block in crystal design, 4,4'-bpno, which may be involved in various connectivity modes (coordinative, hydrogen bond,  $\pi$ – $\pi$  stacking), is able to generate a rich variety of solid-state architectures. Its potentialities deserve to be further exploited.

## 6. A flexible *N,N'*-*exo*-bidentate ligand: 1,2-bis(4-pyridyl)ethane

In contrast with the rigid *N,N'*-spacers presented above, 1,2-bis(4-pyridyl)ethane (bpeta) may adopt different conformations, namely *gauche* and *anti* (Scheme 27). It acts as a bridging or as a terminal ligand as well, and it is capable to act as a hydrogen bond acceptor. Consequently, one expects, in many systems generated by this ligand, the coexistence of coordinative and non-covalent interactions.

In one compound, [Cd(bpeta)<sub>1.5</sub>(NO<sub>3</sub>)<sub>2</sub>], both conformations for the bridging ligand have been observed (Fig. 24) [53]. The conformational freedom of bpeta generates interesting cases of supramolecular isomerism [54]. Several very interesting solid–solid state architectures are constructed without the intervention of hydrogen bonds or stacking interactions [53–55]. These will be not reviewed here.

Two types of supramolecular architectures based on coordinative and hydrogen bond interactions have been obtained by reacting transition metal perchlorates with bpeta. The first one is found in a series of three isomorphous compounds, [M( $\mu$ -bpeta)(bpeta)<sub>2</sub>(H<sub>2</sub>O)<sub>2</sub>]·(0.5bpeta)(H<sub>2</sub>O)(ClO<sub>4</sub>)<sub>2</sub> (**32**) (M = Co, **32a**; Ni, **32b**; Zn, **32c**) [56a]. Three bpeta molecules are directly bonded to the metal ions in compounds **32**. Only one of them forms a genuine bridge between the metal ions, resulting in infinite linear chains. The two other bpeta molecules are terminal ligands. The metal ions are hexacoordinated by four nitrogen atoms from the bpeta ligands and two *trans* aqua ligands. The bridging bpeta and one of the terminal bpeta molecules exhibit the more stable *antiperiplanar* conformation, while the other one is frozen into the *gauche* conformation. Each *gauche*-bpeta molecule of one chain is hydrogen bonded to one aqua ligand from a second chain, this one 'embraces' in the same way a third chain and so on, resulting in

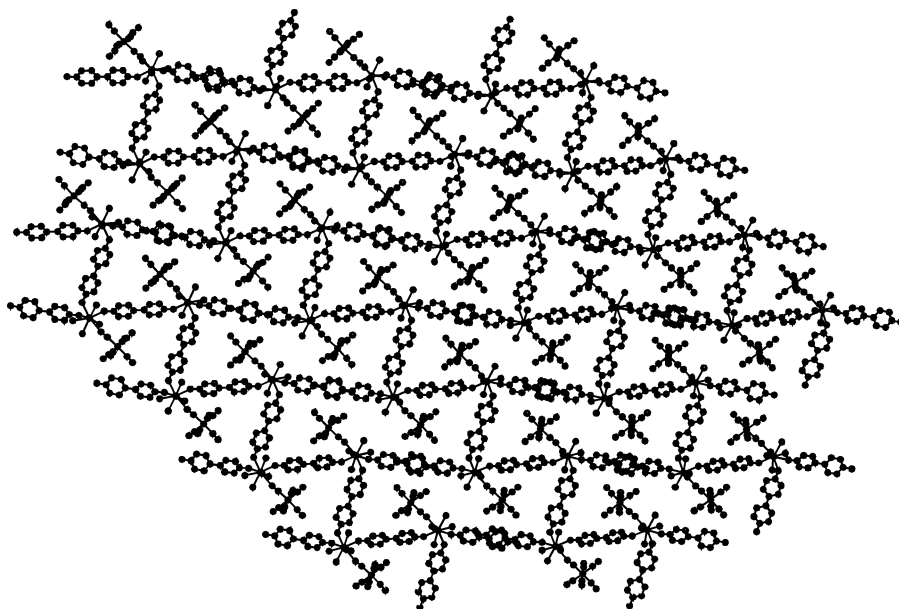


Fig. 22. Packing diagram of compounds **31**, showing the brick wall-like backbone resulting from  $\pi$ - $\pi$  stacking interactions between the terminal ligands belonging to different chains (adapted from Ref. [52]).

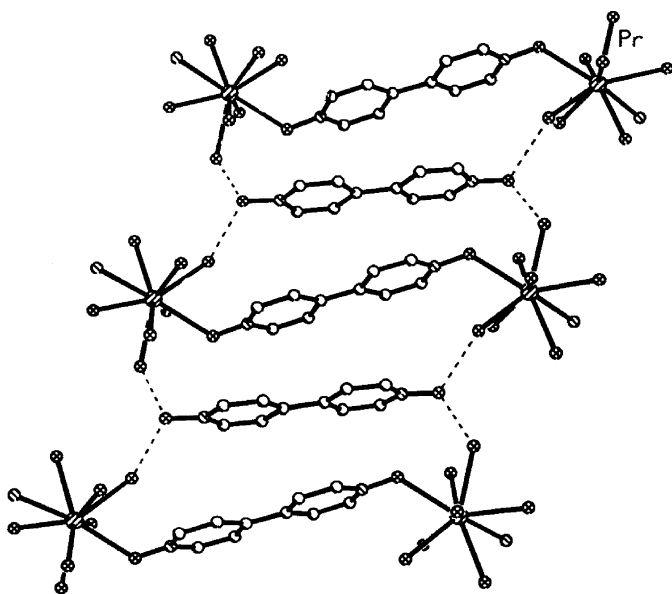


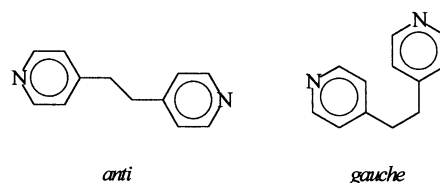
Fig. 23. Hydrogen bond interactions between the uncoordinated 4,4'-bpno molecule and four aqua ligands arising from two different chains in compounds **31** (adapted from Ref. [52]).

infinite layers). Two neighboring layers run in opposite directions (Fig. 25). Each layer is interconnected to left and right adjacent layers through hydrogen bonds established between the *anti*-bpeta terminal ligand from one layer and the aqua ligand from another layer and vice versa, resulting in a 3-D network with large channels (Fig. 26). One type of channels is occupied by pairs of terminal *gauche*-bpeta ligands belonging to neighboring chains, as well as by perchlo-

rate anions. The peripheral pyridyl moieties interact through  $\pi$ - $\pi$  stacking. The other type of channels is occupied by solvated uncoordinated bpeta guests and perchlorate anions.

The anion seems to be playing a key role in stabilizing the solid-state architectures of Co(II) complexes with bpeta. Compound **32a** and that reported by Ciani and co-workers,  $[\text{Co}_5(\text{bpeta})_9(\text{H}_2\text{O})_8(\text{SO}_4)_4](\text{SO}_4) \cdot 14\text{H}_2\text{O}$  **55c**, are obtained under similar conditions (water/ethanol solutions) the first one from  $\text{Co}(\text{ClO}_4)_2 \cdot 6\text{H}_2\text{O}$ , and the other one from  $\text{CoSO}_4 \cdot 7\text{H}_2\text{O}$ . In the sulfato derivative, the  $\text{SO}_4^{2-}$  ions are coordinated to the cobalt ions. The nitrate derivatives, reported by Zaworotko and co-workers [54a], have been obtained differently (organic solvents and the presence of templating agents).

The other structural type is illustrated by one compound:  $[\text{Mn}(\text{bpeta})(\text{H}_2\text{O})_4](\text{ClO}_4)_2 \cdot 4(\text{bpeta}) \cdot 2\text{H}_2\text{O}$  (**33**) [56b], which exhibits an unprecedented interpenetrating mode. Its structure consists of linear  $\text{Mn}-\mu\text{-bpeta}-\text{Mn}-\mu\text{-bpeta}-$  chains, each manganese ion being hexacoordinated by two nitrogen atoms from the bridging bpeta molecules and four aqua ligands. The other four bpeta molecules are not coordinated to the metal atoms, but are involved in an interesting extensive hydrogen bonding system. Each aqua ligand is hydrogen



Scheme 27.

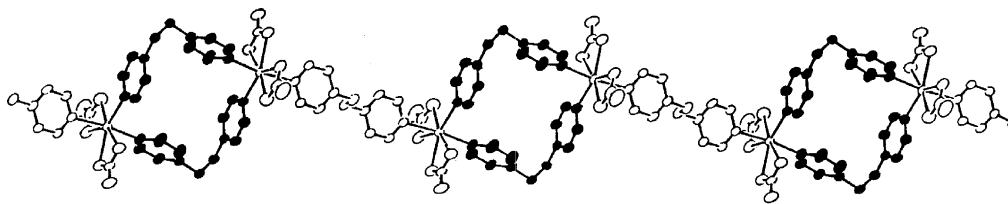
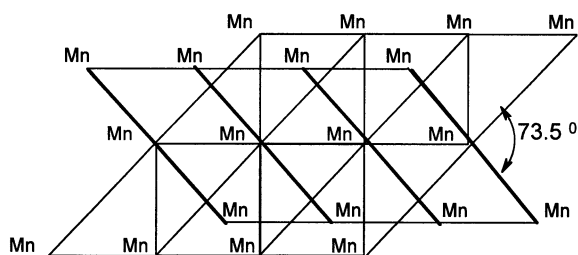


Fig. 24. View of a 1-D polymer,  $\{[\text{Cd}(\mu\text{-bpeta})_3](\text{NO}_3)_2\}_n$  resulting from bridging *gauche*- (drawn in black) and *anti*-bpeta molecules (adapted from Ref. [53a]).

bonded to two nitrogen atoms arising from the organic molecules. There are intra- and interchain hydrogen bonds, which represent the most intriguing feature of the crystal structure of this compound. Two *trans* aqua ligands from one manganese atom are ‘bridged’ through intrachain hydrogen bonds, by two bpeta molecules, to the equivalent aqua ligands on the next manganese atom along the chain. These two bpeta molecules together with the bridging one form infinite triple chains (Fig. 27). The other two aqua ligands are then interchain hydrogen bonded, via the fourth and the fifth bpeta molecules, resulting in two equivalent interpenetrating infinite 2-D chicken-wire sheets (Fig. 28). The hexagonal meshes have two short and four long edges: the short ones (4.29 Å) represent the O–Mn–O distance, while each of the four long edges (14.65 and 14.75 Å) is formed by one bpeta molecule that is hydrogen bonded to two aqua ligands belonging to two different chains.

Another Mn(II) compound has been obtained by assembling  $\text{Mn}^{2+}(\text{aq})$  cations with bpeta and the terephthalate (tp) anion:  $[\text{Mn}(\text{bpeta})(\text{H}_2\text{O})_4](\text{tp}) \cdot 2(\text{bpeta})$  (**34**) [57]. The Mn(II) ions are bridged by bpeta ligands resulting in infinite chains, like in compound **33**. The tp anions are not coordinated to the metal ions, but play, together with the uncoordinated bpeta molecules, an important role in increasing the dimensionality through hydrogen bonds. All eight hydrogen atoms from the four aqua ligands are involved in hydrogen bond interactions with four bpeta molecules and two terephthalate anions (Figs. 29 and 30). The resulting architecture can be described as being formed by two intersecting sheets. The first one results from the interconnection of the chains by the hydrogen bonded terephthalate anions. The other one results in the same manner, but via hydrogen bonded bpeta molecules. The

dihedral angle between the two sheets is  $73.5^\circ$  (Scheme 28). The magnetic properties of **34** have been investigated down to 1.8 K. The weak antiferromagnetic behavior is ascribed to the intrachain exchange interaction of the Mn(II) ions ( $J = -0.84 \text{ cm}^{-1}$ ). Most probably, both intra- and interchain exchange pathways are operative here.



Scheme 28.

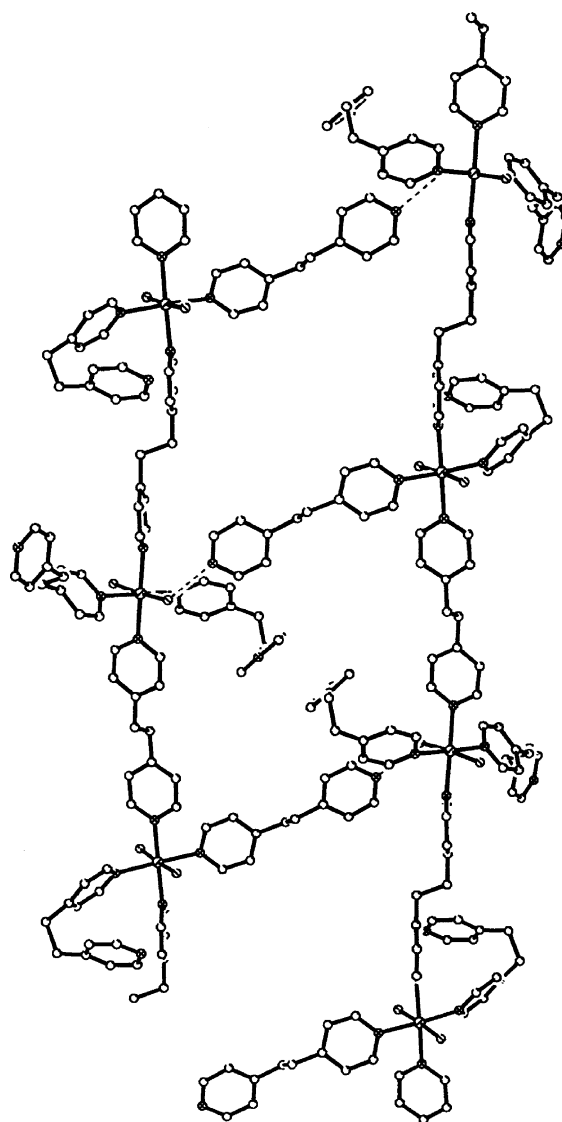


Fig. 25. Hydrogen bond cross-linkages of chains belonging to different layers in compounds **32**, through the terminal *anti*-bpeta ligands (adapted from Ref. [56a]).



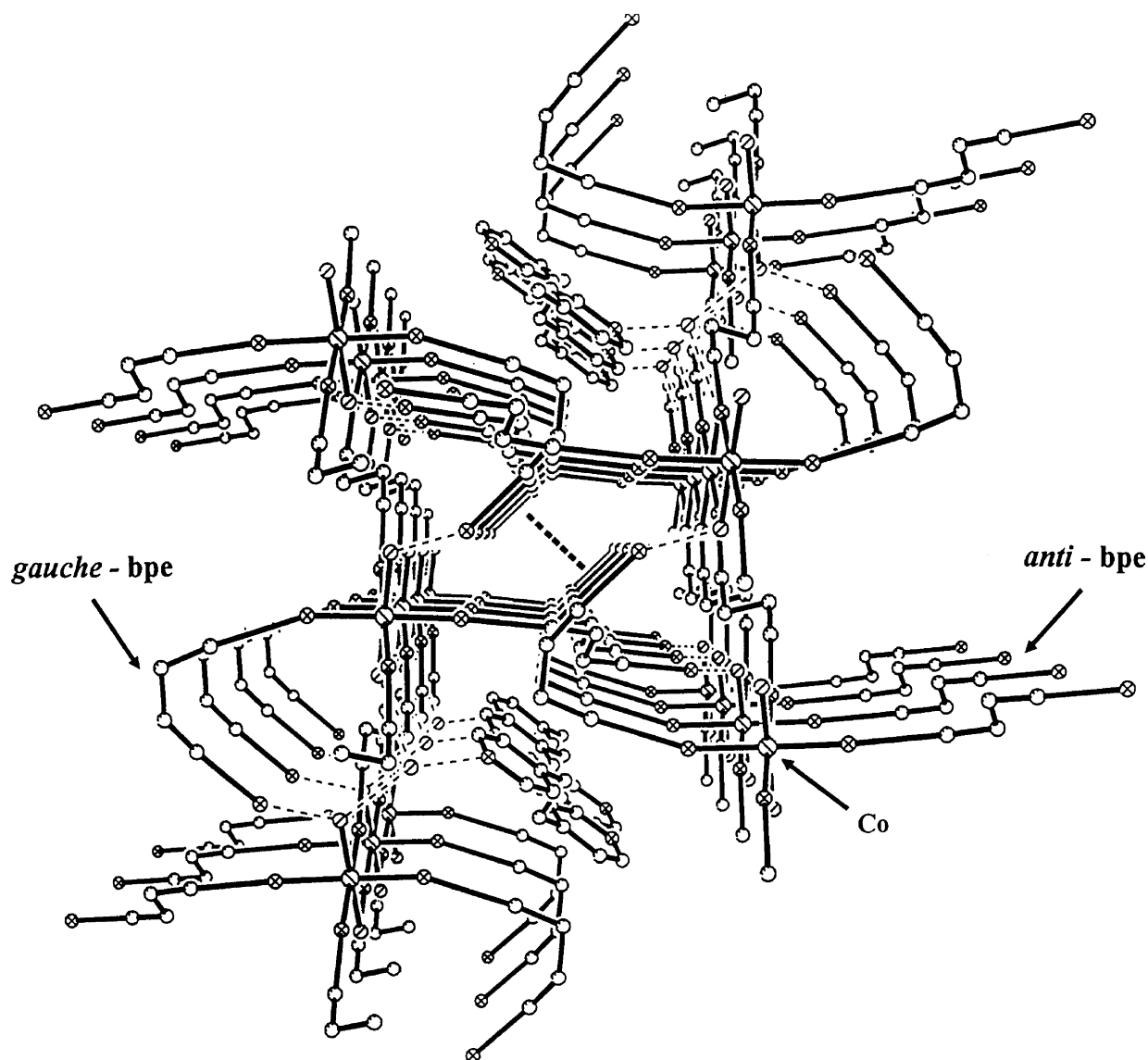


Fig. 26. Projection of the 3-D architecture of compounds **32**, looking down the microchannels. For clarity, the bpeta molecules, except the uncoordinated ones, are represented by lines and the perchlorate anions are omitted (adapted from Ref. [56a]).

The reaction of compound **33** with dipotassium terephthalate leads to another terephthalato–bpeta derivative:  $[\text{Mn}(\text{bpeta})_{1.5}(\text{H}_2\text{O})(\text{tp})] \cdot \text{H}_2\text{O}$  [58], which is a 3-D coordination polymer, in which the Mn(II) ions are bridged by both bpeta and tp ligands. One bpeta

molecule, with the *anti* conformation, acts as a bridge, while the terminal one has the *gauche* conformation.

The self-assembly process between Zn(II) ions, isophthalate (bdc) and bpeta in ethanol and in the presence of an appropriately sized guest afforded a puckered,

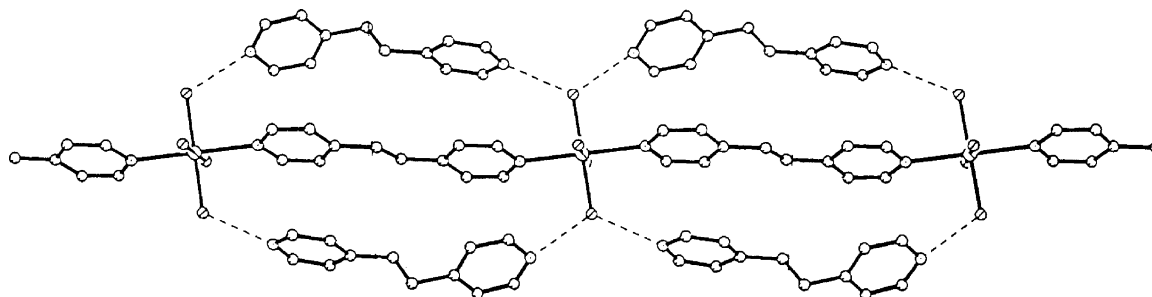


Fig. 27. Infinite 'triple' chains in compound **33**.

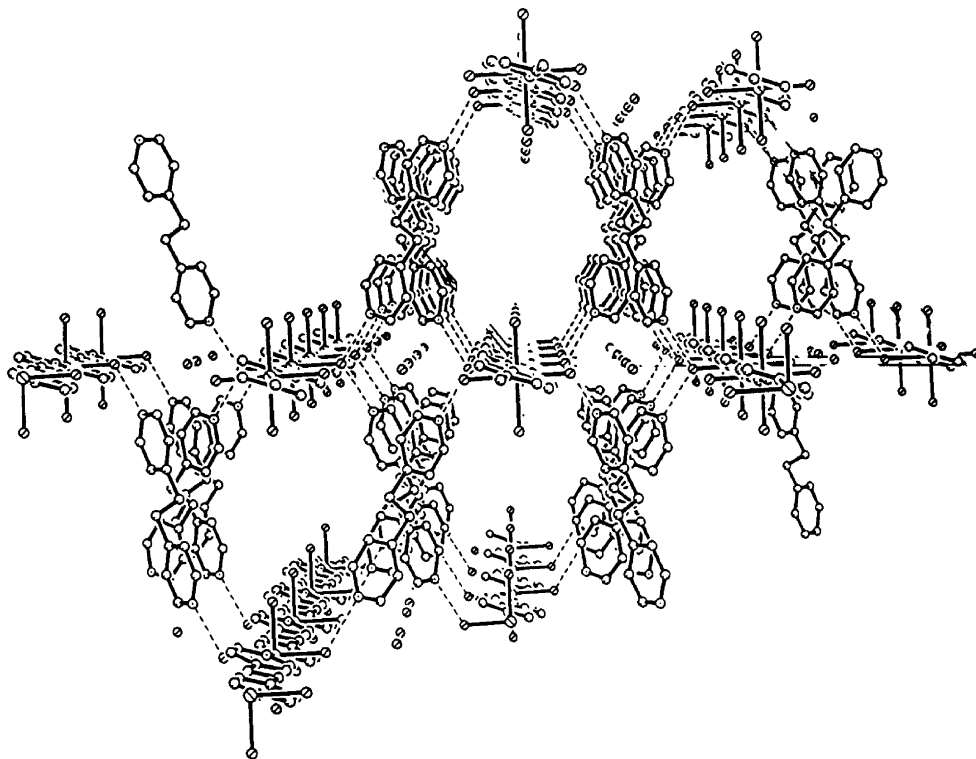


Fig. 28. Packing diagram for compound 33, showing the interpenetrating layers.

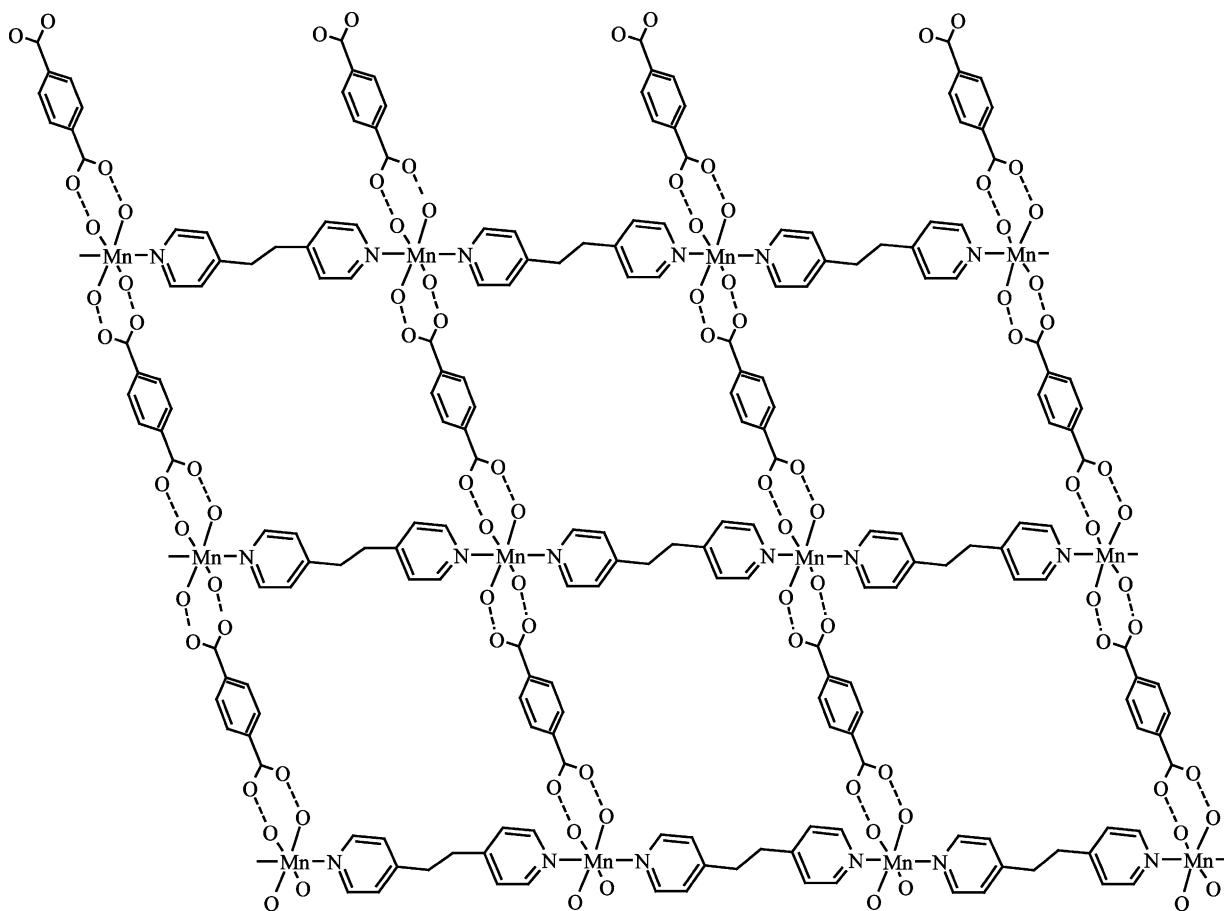


Fig. 29. The formation of a sheet in compound 34 by interconnecting the chains through hydrogen bonded terephthalate ions.

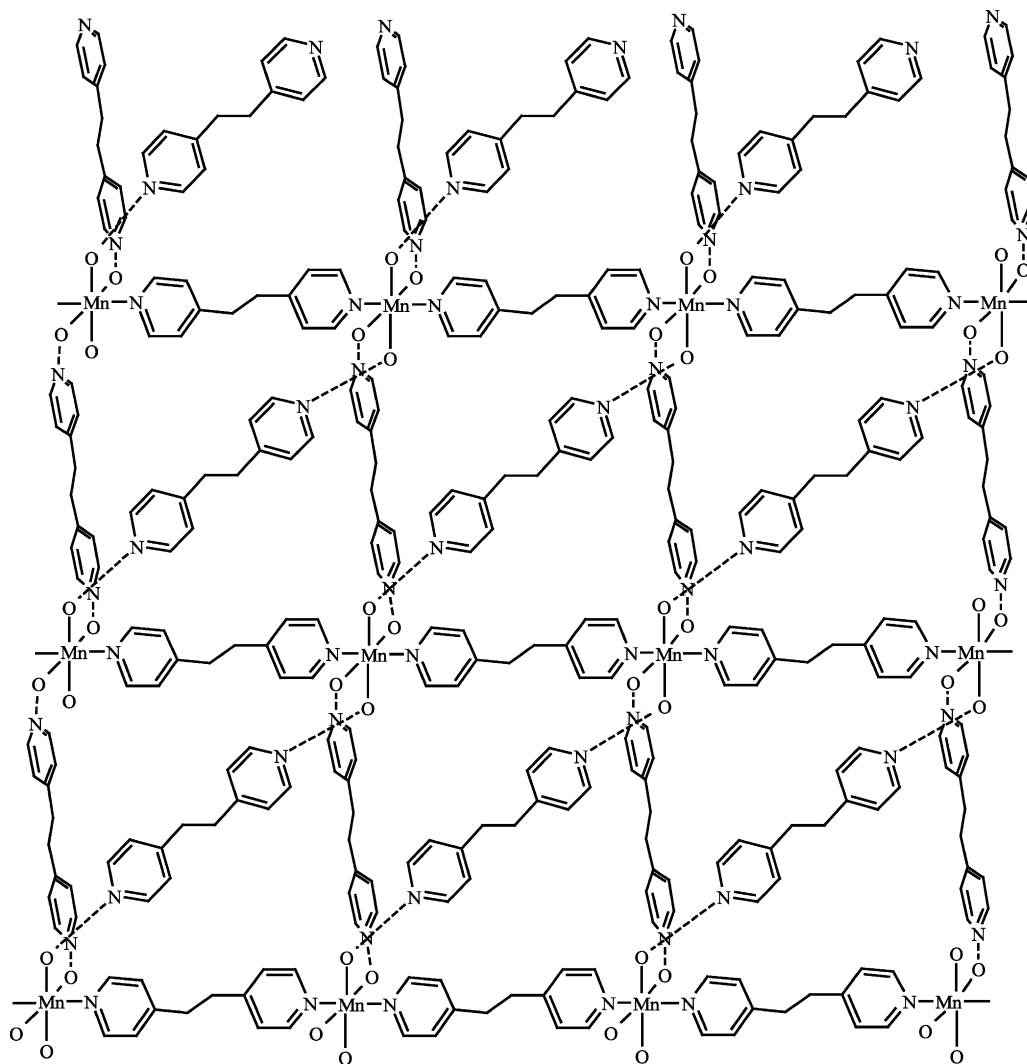
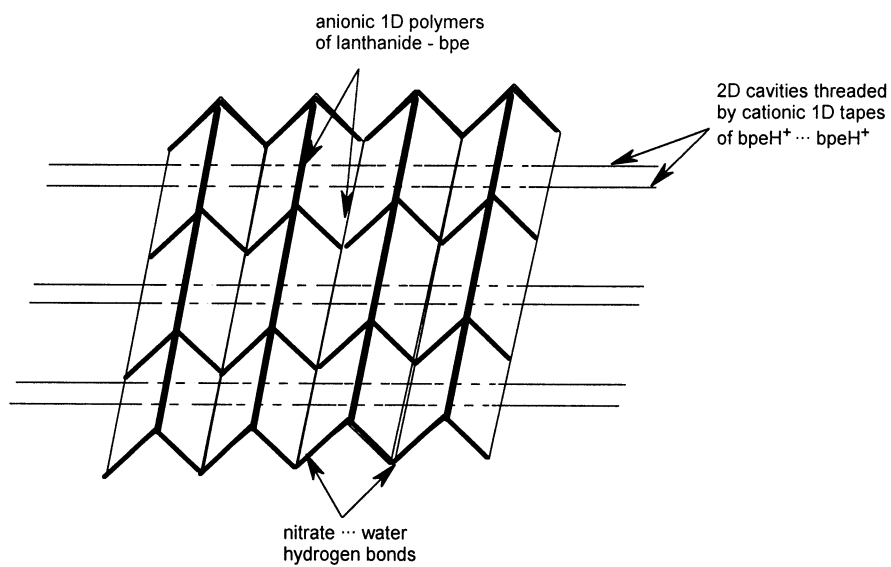


Fig. 30. The formation of a sheet in compound **34** by interconnecting the chains through hydrogen bonded bpe<sub>2</sub> molecules.



Scheme 29.

rectangular grid structure,  $[\text{Zn}(\text{bpeta})(\text{bdc})]_n \cdot x\text{G}$  (**35**), where the guest molecules are: benzene, toluene, nitrobenzene, benzaldehyde, 1,4-dioxane [59]. By changing the solvent, and working without guest molecules, a supramolecular isomer of **35**, with a 3-D structure, is obtained. The coordinative network in **35** is sustained by tetrahedral Zn(II) ions, which are bridged by two bpeta and two bdc ligands. The guest molecules form a non-covalent ‘puckered brick wall’ network, which is engaged in a parallel interpenetration with the coordination polymer. A similar situation, showing interpenetrating covalent and non-covalent networks, was found in the case of compound **15**.

As in the case of 4,4'-bipy, the chemistry of bpeta with lanthanide(III) ions is scarce. Only one compound with bpeta bridges has been reported [38a]:  $(\text{Hbpeta})[\text{La}(\text{NO}_3)_4(\text{H}_2\text{O})_2(\mu\text{-bpeta})]$  (**36**). Compound **36** crystallizes in the chiral space group  $C22_1$ , confirming the supposition that lanthanide cations are good candidates for constructing chiral networks. The lanthanum(III) ions are 11-coordinated (four bidentate nitrato groups, two nitrogen atoms arising from the bridging bpeta molecules and one aqua ligand). The lanthanum ions are bridged by bpeta ligands, leading to infinite anionic chains. The chains are further interconnected by hydrogen bonds established between one water molecule and the nitrato groups from another chain, resulting in a pleated-sheet structure with cavities (molecular ‘Chinese blinds’). Each cavity is threaded by two linear hydrogen bonded chains of monoprotonated,  $\text{Hbpeta}^+$ , molecules, resulting in an interesting polypseudo-rotaxane architecture (Scheme 29).

## 7. Conclusions and perspectives

The bipy-type  $N,N'$  and  $O,O'$  ligands discussed here are able to further generate an extremely rich solid-state chemistry. The utilization of the 4d and 5d transition metal ions as nodes in designing extended structures remains largely unexploited. There are only a few attempts to obtain heterobimetallic assemblies by using these molecules as linkers and spacers. Such systems could exhibit interesting magnetic, electric, optical or catalytic properties.

Although most of the structures reviewed here in could not be predicted, they pave the way towards the rational level in designing crystals. Some others illustrate how the convolution of metal–ligand bonds with weak non-covalent interactions may lead to robust superstructures with desired properties (e.g. nanoporosity, solid-state reactivity, magnetism, NLO activity).

The interplay of coordination bonds with various and rather weak interactions (hydrogen bonding,  $\pi$ – $\pi$  stacking, secondary bonds [60]), plus the electrostatic Madelung lattice energy hinder the strict control over the

crystal packing. The presence of the solvent molecules in the crystals is sometimes a drawback, since these may infer with the pre-selected set of intermolecular interactions leading to undesired networks. Despite all these, we must keep opened the door to the compounds obtained by serendipity: they may exhibit not only surprising and unprecedented structures, but also useful properties.

## Acknowledgements

M.A. is grateful to the Alexander von Humboldt Foundation for the financial support of his stay in Germany (April–July 2001).

## References

- [1] (a) D. Venkataraman, G.B. Gardner, S. Lee, J.S. Moore, *J. Am. Chem. Soc.* 117 (1995) 11600;  
(b) O.M. Yaghi, G. Li, H. Li, *Nature* 378 (1995) 703;  
(c) C.J. Kepert, M.J. Rosseinsky, *Chem. Commun.* (1999) 375;  
(d) K. Biradha, Y. Hongo, M. Fujita, *Angew. Chem. Int. Ed. Engl.* 39 (2000) 3843;  
(e) M. Eddaoudi, D.B. Moler, H. Li, B. Chen, T.M. Reinecke, M. O’Keeffe, O.M. Yaghi, *Acc. Chem. Res.* 34 (2001) 319;  
(f) K. Seiki, S. Takamizawa, W. Mori, *Chem. Lett.* (2001) 332.
- [2] M. Fujita, Y.J. Kwon, S. Washizu, K. Ogura, *J. Am. Chem. Soc.* 116 (1994) 1151.
- [3] See for example: (a) O. Kahn, *Molecular Magnetism*, VCH, New York, 1993;  
(b) J.S. Miller, A.J. Epstein, *Angew. Chem. Int. Ed. Engl.* 33 (1994) 385;  
(c) M. Ohba, H. Okawa, *Coord. Chem. Rev.* 198 (2000) 313;  
(d) K.R. Dunbar, R.A. Heintz, *Progr. Inorg. Chem.* 45 (1997) 283;  
(e) E. Coronado, J.R. Galán-Mascarós, C.J. Gómez-García, J. Ensling, P. Gülich, *Chem. Eur. J.* 6 (2000) 552;  
(f) H.O. Stumpf, L. Ouahab, Y. Pei, P. Bergerat, O. Kahn, *J. Am. Chem. Soc.* 116 (1994) 3866;  
(g) E. Coronado, M. Clemente-León, J.R. Galán-Mascarós, C. Giménez-Saiz, C.J. Gómez-García, E. Martínez-Ferrero, *J. Chem. Soc. Dalton Trans.* (2000) 3955.
- [4] (a) J.-M. Lehn, *Science* 260 (1993) 1762;  
(b) B.J. Holliday, C.A. Mirkin, *Angew. Chem. Int. Ed. Engl.* 40 (2001) 2022.
- [5] R.W. Gable, B.F. Hoskins, R. Robson, *J. Chem. Soc. Chem. Commun.* (1990) 1677.
- [6] (a) M. Andruh, H.W. Roesky, M. Noltemeyer, H.-G. Schmidt, *Z. Naturforsch. Teil b* 49 (1994) 31;  
(b) J. Lu, C. Yu, T. Niu, T. Paliwala, G. Crisci, F. Somosa, A.J. Jacobson, *Inorg. Chem.* 37 (1998) 4637;  
(c) A.S. Batsanov, M.J. Begley, P. Hubberstey, J. Stroud, *J. Chem. Soc. Dalton Trans.* (1996) 1947;  
(d) C. Chen, D. Xu, Y. Xu, C. Cheng, *Acta Crystallogr. Sect. C* 48 (1992) 1231.
- [7] See for example: (a) L.R. MacGillivray, S. Subramanian, M.J. Zaworotko, *J. Chem. Soc. Chem. Commun.* (1994) 1325;  
(b) L. Carlucci, G. Ciani, D.M. Proserpio, A. Sironi, *J. Chem. Soc. Chem. Commun.* (1994) 2755;  
(c) T. Kuroda-Sowa, M. Yamamoto, M. Munakata, M. Seto, M. Maekawa, *Chem. Lett.* (1996) 349.

- [8] See for example: S. Subramanian, M.J. Zaworotko, *Angew. Chem. Int. Ed. Engl.* 34 (1995) 2127.
- [9] (a) O.M. Yaghi, H. Li, C. Davis, D. Richardson, T.L. Groy, *Acc. Chem. Res.* 31 (1998) 474;  
(b) S. Kitagawa, M. Kondo, *Bull. Chem. Soc. Jpn.* 71 (1998) 1739;  
(c) S.R. Batten, R. Robson, *Angew. Chem. Int. Ed. Engl.* 37 (1998) 1460;  
(d) P.J. Hagram, D. Hagram, J. Zubieta, *Angew. Chem. Int. Ed. Engl.* 38 (1999) 2638;  
(e) M.J. Zaworotko, *Chem. Commun.* (2001) 1;  
(f) R. Robson, *J. Chem. Soc. Dalton Trans.* (2000) 3735;  
(g) A.N. Khlobystov, A.J. Blake, N.R. Champness, D.A. Lemenovskii, A.G. Majouga, N.V. Zyk, M. Schröder, *Coord. Chem. Rev.* 222 (2001) 155.
- [10] (a) M.C. Etter, *Acc. Chem. Res.* 23 (1990) 120;  
(b) S. Subramanian, M.J. Zaworotko, *Coord. Chem. Rev.* 137 (1994) 357.
- [11] (a) J.C. MacDonald, G.M. Whitesides, *Chem. Rev.* 94 (1994) 2383;  
(b) C.B. Aakeröy, K.R. Seddon, *Chem. Rev.* 93 (1993) 397;  
(c) G.R. Desiraju, in: F. Vögtle, J.F. Stoddart, M. Shibasaki (Eds.), *Stimulating Concepts in Chemistry*, Wiley VCH, Weinheim, 2000, p. 293.
- [12] J.W. Steed, J.L. Atwood, *Supramolecular Chemistry*, Wiley, Chichester, 2000.
- [13] W.L. Jorgensen, D.L. Severance, *J. Am. Chem. Soc.* 112 (1990) 4768.
- [14] C. Janiak, *J. Chem. Soc. Dalton Trans.* (2000) 3885.
- [15] (a) G. Marinescu, M. Andruh, R. Lescouëzec, M.C. Muñoz, J. Cano, F. Lloret, M. Julve, *New J. Chem.* 24 (2000) 527;  
(b) M.C. Muñoz, M. Julve, F. Lloret, J. Faus, M. Andruh, *J. Chem. Soc. Dalton Trans.* (1998) 3125.
- [16] S.F. Lai, C.Y. Chen, K.J. Lin, *Chem. Commun.* (2001) 1082.
- [17] (a) K.S. Min, M.P. Suh, *Eur. J. Inorg. Chem.* (2001) 449;  
(b) M. Munakata, J. Dai, M. Maekawa, T. Kuroda-Sowa, J. Fukui, *J. Chem. Soc. Chem. Commun.* (1994) 2331.
- [18] (a) C.V.K. Sharma, M.J. Zaworotko, *Chem. Commun.* (1996) 2655;  
(b) K. Sivashankar, V.R. Pedireddi, C.N.R. Rao, *J. Mol. Struct.* 559 (2001) 41;  
(c) V.R. Pedireddi, S. Chatterjee, A. Ranganathan, C.N.R. Rao, *J. Am. Chem. Soc.* 119 (1997) 10867;  
(d) A. Ranganathan, V.R. Pedireddi, G. Sanjayan, K.N. Ganesh, C.N.R. Rao, *J. Mol. Struct.* 522 (2000) 87;  
(e) S.B. Copp, S. Subramanian, M.J. Zaworotko, *Angew. Chem. Int. Ed. Engl.* 32 (1993) 706.
- [19] C. He, B.G. Zhang, C.Y. Duan, J.H. Li, Q.J. Meng, *Eur. J. Inorg. Chem.* (2000) 2549.
- [20] (a) J.F. Létard, P. Guionneau, E. Codjovi, O. Lavastre, G. Bravic, D. Chasseau, O. Kahn, *J. Am. Chem. Soc.* 119 (1997) 10861;  
(b) J.F. Létard, P. Guionneau, L. Rabardel, J.A.K. Howard, A.E. Goeta, D. Chasseau, O. Kahn, *Inorg. Chem.* 37 (1998) 4432;  
(c) M. Wesolek, D. Meyer, J.A. Osborn, A. De Cian, J. Fisher, A. Derory, P. Logoll, M. Drillon, *Angew. Chem. Int. Ed. Engl.* 33 (1994) 1592;  
(d) A.J. Amoroso, J.C. Jeffery, P.L. Jones, J.A. McCleverty, P. Thornton, M.D. Ward, *Angew. Chem. Int. Ed. Engl.* 34 (1995) 1443.
- [21] L. Carlucci, G. Ciani, D.M. Proserpio, A. Sironi, *J. Chem. Soc. Dalton Trans.* (1997) 1801.
- [22] A.J. Blake, S.J. Hill, P. Hubberstey, W.S. Li, *J. Chem. Soc. Dalton Trans.* (1997) 913.
- [23] X.M. Chen, M.L. Tong, Y.J. Luo, Z.N. Chen, *Aust. J. Chem.* 49 (1996) 835.
- [24] S.D. Huang, R.G. Xiong, *Polyhedron* 16 (1997) 3929.
- [25] M.X. Li, G.Y. Xie, Y.D. Gu, J. Chen, P.J. Zheng, *Polyhedron* 14 (1995) 1235.
- [26] S. Noro, M. Kondo, T. Ishii, S. Kitagawa, H. Matsuzaka, *J. Chem. Soc. Dalton Trans.* (1999) 1569.
- [27] J. Lu, T.P. Shiao, C. Yu, T. Niu, A.J. Jacobson, *Inorg. Chem.* 36 (1997) 923.
- [28] G. De Munno, D. Armentano, T. Poerio, M. Julve, J.A. Real, *J. Chem. Soc. Dalton Trans.* (1999) 1813.
- [29] M. Andruh, in: G. Ondrejovic, A. Sirota (Eds.), *Coordination Chemistry at the Turn of the Century*, STU Press, Bratislava, 1999, p. 31.
- [30] (a) M.L. Tong, B.H. Ye, J.W. Cai, X.M. Chen, S.W. Ng, *Inorg. Chem.* 37 (1998) 2645;  
(b) M.L. Tong, S.L. Zheng, X.M. Chen, *Polyhedron* 19 (2000) 1809.
- [31] K. Biradha, K.V. Domasevitch, B. Moulton, C. Seward, M.J. Zaworotko, *Chem. Commun.* (1999) 1327.
- [32] O.M. Yaghi, H. Li, T.L. Groy, *Inorg. Chem.* 36 (1997) 4292.
- [33] M.L. Tong, H.K. Lee, X.M. Chen, R.B. Huang, T.C.W. Mak, *J. Chem. Soc. Dalton Trans.* (1999) 3657.
- [34] (a) M.L. Tong, X.M. Chen, X.L. Yu, T.C.W. Mak, *J. Chem. Soc. Dalton Trans.* (1998) 5;  
(b) L.M. Zheng, X. Fang, K.H. Lii, H.H. Song, X.Q. Xin, H.K. Fun, K. Chinnakali, I.A. Razak, *J. Chem. Soc. Dalton Trans.* (1999) 231;  
(c) J. Lu, C. Yu, T. Niu, T. Paliwala, G. Crisci, F. Somosa, A.J. Jacobson, *Inorg. Chem.* 37 (1998) 4637;  
(d) Y.S. Zhang, G.D. Enright, S.R. Breeze, S. Wang, *New J. Chem.* 23 (1999) 625;  
(e) Z. Shi, L. Zhang, S. Gao, G. Yang, J. Hua, L. Gao, S. Feng, *Inorg. Chem.* 39 (2000) 1990;  
(f) J. Li, H. Zeng, J. Chen, Q. Wang, X. Wu, *Chem. Commun.* (1997) 1213; Y. Rodriguez-Martin, C. Ruiz-Pérez, J. Sanchiz, F. Lloret, M. Julve, *Inorg. Chim. Acta* 318 (2001) 159;  
(g) L.R. MacGillivray, R.H. Groeneman, J.L. Atwood, *J. Am. Chem. Soc.* 120 (1998) 2676;  
(h) B.W. Sun, B.Q. Ma, Z.M. Wang, *New J. Chem.* 24 (2000) 853;  
(i) J. Tao, M.L. Tong, J.X. Shi, X.M. Chen, S.W. Ng, *Chem. Commun.* (2000) 2043;  
(j) J. Tao, M.L. Tong, X.M. Chen, *J. Chem. Soc. Dalton Trans.* (2000) 3669;  
(k) L. Pan, N. Ching, X. Huang, J. Li, *Chem. Commun.* (2001) 1064;  
(l) Q. Wang, X. Wu, W. Zhang, T. Sheng, P. Lin, J. Li, *Inorg. Chem.* 38 (1999) 2223;  
(m) A.M. Chippindale, A.R. Cowley, K.J. Peacock, *Acta Crystallogr. Sect. C* 56 (2000) 651;  
(n) S.R. Batten, B.F. Hoskins, R. Robson, *Chem. Eur. J.* 6 (2000) 156;  
(o) C.H. Huang, L.H. Huang, K.H. Lii, *Inorg. Chem.* 40 (2001) 2625;  
(p) H. Hou, Y. Wei, Y. Fan, C. Du, Y. Zhu, Y. Song, Y. Niu, X. Xin, *Inorg. Chim. Acta* 319 (2001) 212.
- [35] M.L. Tong, H.J. Chen, X.M. Chen, *Inorg. Chem.* 39 (2000) 2235.
- [36] (a) F. Robinson, M.J. Zaworotko, *J. Chem. Soc. Chem. Commun.* (1995) 2413;  
(b) K.N. Power, T.L. Hennigar, M.J. Zaworotko, *New J. Chem.* (1998) 177.
- [37] M. Bukowska-Strzyzewska, A. Tosik, *Inorg. Chim. Acta* 30 (1978) 189.
- [38] (a) C.V. Krishnamohan Sharma, R.D. Rogers, *Chem. Commun.* (1999) 83;  
(b) K.T. Al-Rasoul, M.G.B. Drew, *Acta Crystallogr. Sect. C* 43 (1987) 2081.
- [39] K.T. Al-Rasoul, T.J.R. Weakley, *Inorg. Chim. Acta* 63 (1982) 161.
- [40] T.J.R. Weakley, *Inorg. Chim. Acta* 95 (1984) 317.



- [41] V.A. Trush, J. Swiatek-Kozłowska, V.V. Skopenko, V.M. Amyrkhanov, Z. Naturforsch. Teil b 56 (2001) 249.
- [42] C. Seward, N.X. Hu, S. Wang, J. Chem. Soc. Dalton Trans. (2001) 134.
- [43] (a) C.Y. Su, B.S. Kang, H.Q. Liu, Q.G. Wang, T.C.W. Mak, Chem. Commun. (1998) 1551;  
(b) C.Y. Su, B.S. Kang, Q.C. Yang, T.C.W. Mak, J. Chem. Soc. Dalton Trans. (2000) 1857.
- [44] (a) A.L. Gillon, G.R. Lewis, A.G. Orpen, S. Rotter, J. Starbuck, X.M. Wang, Y. Rodríguez-Martín, C. Ruiz-Pérez, J. Chem. Soc. Dalton Trans. (2000) 3897;  
(b) L.J. Barbour, L.R. MacGillivray, J.L. Atwood, Supramol. Chem. 7 (1996) 167.
- [45] H.J. Chen, L.Z. Zhang, Z.G. Cai, G. Yang, X.M. Chen, J. Chem. Soc. Dalton Trans. (2000) 2463.
- [46] (a) M.J. Plater, M.R. St.J. Foreman, A.M.Z. Slawin, Inorg. Chim. Acta 303 (2000) 132;  
(b) S. Bruda, M. Andruh, H.W. Roesky, Y. Journaux, M. Noltemeyer, E. Rivière, Inorg. Chem. Commun. 4 (2001) 111.
- [47] (a) B.Q. Ma, S. Gao, H.L. Sun, G.X. Xu, J. Chem. Soc. Dalton Trans. (2001) 130;  
(b) B.Q. Ma, H.L. Sun, S. Gao, G.X. Xu, Inorg. Chem. 40 (2001) 6247.
- [48] D.L. Long, A.J. Blake, N.R. Champness, M. Schröder, Chem. Commun. (2000) 2273.
- [49] D. Visinescu, G.I. Pascu, M. Andruh, J. Magull, H.W. Roesky, Inorg. Chim. Acta, in press.
- [50] A. Nedelcu, Z. Žák, A.M. Madalan, J. Pinkas, M. Andruh, unpublished.
- [51] (a) D.L. Long, A.J. Blake, N.R. Champness, M. Schröder, Chem. Commun. (2000) 1369;  
(b) D.L. Long, A.J. Blake, N.R. Champness, C. Wilson, M. Schröder, J. Am. Chem. Soc. 123 (2001) 3401.
- [52] S. Tanase, M. Andruh, A. Müller, M. Schmidtman, C. Mathonière, G. Rombaut, Chem. Commun. (2001) 1084.
- [53] (a) M. Fujita, Y.J. Kwon, M. Miyazawa, K. Ogura, J. Chem. Soc. Chem. Commun. (1994) 1977;  
(b) M. Fujita, M. Aoyaghi, K. Okura, Bull. Chem. Soc. Jpn. 71 (1998) 1799.
- [54] (a) T.L. Hennigar, D.C. MacQuarrie, P. Loisier, R.D. Rogers, M.J. Zaworotko, Angew. Chem. Int. Ed. Engl. 36 (1997) 972;  
(b) B. Moulton, M.J. Zaworotko, Chem. Rev. 101 (2001) 1629.
- [55] Networks constructed from both bpeta molecules and bridging anions: (a) K.N. Power, T.L. Hennigar, M.J. Zaworotko, Chem. Commun. (1998) 595;  
(b) Q.M. Wang, G.C. Guo, T.C.W. Mak, Chem. Commun. (1999) 1849;  
(c) L. Carlucci, G. Ciani, D.M. Proserpio, S. Rizzato, Chem. Commun. (2000) 1319;  
(d) Y.B. Dong, R.C. Layland, M.D. Smith, N.G. Pschirer, U.H.F. Bunz, H.C. zur Loe, Inorg. Chem. 38 (1999) 3056;  
(e) M.L. Hernández, M. Gotzone Barandika, M.K. Urtiaga, R. Cortés, L. Lezama, M.I. Arruortua, J. Chem. Soc. Dalton Trans. (2000) 79.
- [56] (a) M. Ferbinteanu, G. Marinescu, H.W. Roesky, M. Noltemeyer, H.G. Schmidt, M. Andruh, Polyhedron 18 (1999) 243;  
(b) F.D. Rochon, M. Andruh, R. Melanson, Can. J. Chem. 76 (1998) 1564.
- [57] C.S. Hong, Y. Do, Inorg. Chem. 37 (1998) 4470.
- [58] C.S. Hong, S.K. Son, Y.S. Lee, M.J. Jun, Y. Do, Inorg. Chem. 38 (1999) 5602.
- [59] S.A. Bourne, J. Lu, B. Moulton, M.J. Zaworotko, Chem. Commun. (2001) 861.
- [60] I. Haiduc, F.T. Edelmann, Supramolecular Organometallic Chemistry, Wiley-VCH, Weinheim, 1999.